Improved *in vitro* Intestinal Epithelial Model with Synthetic Intestinal Mucin

A thesis submitted by

Gautham Salgam

in partial fulfillment of the requirements for the degree of

Master of Science

In

Biomedical Engineering

Tufts University

February 2025

Advisor: **Dr. Ying Chen**

Thesis Committee: **Dr. David Kaplan** (Committee Chair)**, Dr. Ying Chen, Dr. Nikhil Nair**

1. Abstract

The intestine plays an essential role in digestion and immune defense. Atop the small intestinal epithelium sits a thin mucus layer. This layer serves many functions, such as being a physical barrier between the epithelium and luminal contents, a selective filter of nutrients and microbes, and a protective layer against pathogenic bacteria. A number of *in vitro* models have mimicked the small intestine using intestinal epithelial cells and microbiota. However, these models lack adequate mucus layer representation, thus limiting their biological relevancy. Mucus produced by epithelial cells *in vitro* suffers from low yield and current synthetic mucus and animal-derived mucus suffer from a lack of biological relevance and biocompatibility. Synthetic mucins of silk-sugar composition were screened in a 2D transwell model for their capacity to protect Caco-2 cells from bacteria infiltration and their capacity to support the co-existence of these cells and commensal bacteria. Results confirmed that Caco-2 cells were compatible with synthetic mucins of silk-sugar composition and that the protective ability of synthetic mucin to prevent bacteria infiltration diminishes over time. However, results were mixed as to whether silk-sugar mucins could fulfill primary screening objectives, due to conflicting data within and between experiments.

1a. Acknowledgments

I would like to thank my advisors Dr. Ying Chen and Dr. David Kaplan for granting me the opportunity to pursue research at the Kaplan laboratory at Tufts University. I greatly appreciate your guidance, knowledge, and encouragement throughout my thesis journey.

I would like to thank Dr. Nikhil Nair for graciously accepting the role of thesis committee member.

I would like to give a special thanks to Sara Rudolph for her mentorship throughout my thesis journey and for helping me hone my lab skills. I greatly appreciate your kindness, patience, and your willingness to answer even the smallest of my concerns.

I would like to thank Dr. Jugal Sahoo for your insights and for taking the time to create and optimize the glycoproteins vital for all my experiments.

I would like to thank the members of the intestine group at Kaplan laboratory for offering their guidance and tuning in to my bi-weekly update presentations.

I would like to thank Esha Bethi, Omar Da'dara, Lilliane Iglesias, Xinxin Li, Karolinny Vieira, and others for being attentive, patient mentees and granting me valuable teaching experience.

I would like to thank the faculty members and employees of SciTech for keeping things running efficiently.

I would like to thank the Tufts biomedical engineering department for providing a friendly and collaborative research environment.

Lastly, I would like to thank my family and close friends for supporting me through my thesis journey and bearing with me, especially through the writing stage of my thesis.

Table of Contents

1b. Abbreviations

AIEC = Adherent-invasive Escherichia coli

AMP = Antimicrobial peptide

ANOVA = Analysis of variance

BSA = Bovine serum albumin

DAPI = 4′,6-diamidino-2-phenylindole

DMEM = Dulbecco's Modified Eagle Medium

EcN = Escherichia coli Nissle 1917

EDC = N-3-Dimethyl amino propyl-N'-ethyl arbodiimide

EDTA = Ethylenediaminetetraacetic acid

FBS = Fetal bovine serum

GA = Glutaraldehyde

Gal = Galactose

GalN = Galactosamine

GalNAc = N-acetylgalactosamine

GFP = Green fluorescent protein

GI = Gastrointestinal tract

GlcNAc = N-acetylglucosamine

HIE = Human intestinal enteroids

LB = Lysogeny broth

MOI = Multiplicity of infection

MTX = Methotrexate

MUC19 = Mucin 19

MUC2 = Mucin 2

MUC5AC = Mucin 5AC

MUC5B = Mucin 5B

MUC6 = Mucin 6

MUC7 = Mucin 7

MUC8 = Mucin 8

MUC9 = Mucin 9

NeuNAc = Sialic acid

NHS = N-Hydroxy Succinimide

PBS = Phosphate buffered saline

PFA = Paraformaldehyde

RPM = Rotations per minute

SEM = Scanning electron microscopy

SF = Silk fibroin

TEER = Trans-epithelial electrical resistance

ZO-1 = Zonula Occludens-1

2. Introduction

2a. The Gastrointestinal Tract and the Small Intestinal Epithelium

The GI tract is a system of organs primarily concerned with the digestion and absorption of nutrients within the body. The stomach, small intestine, and large intestines of the GI tract form a passageway for nutrients to travel from the mouth to the anus. In addition to its primary function of digestion, the GI tract helps maintain bodily homeostasis by supporting immunity, fluid and electrolyte balance, the expulsion of waste, and the detoxification of substances. In the stomach, gastric acids digest nutrients into chyme, which consists of gastric juices and partially digested nutrients [1]. This chyme then enters the small intestine, where 90% of digestion and absorption of nutrients occurs in the human body.

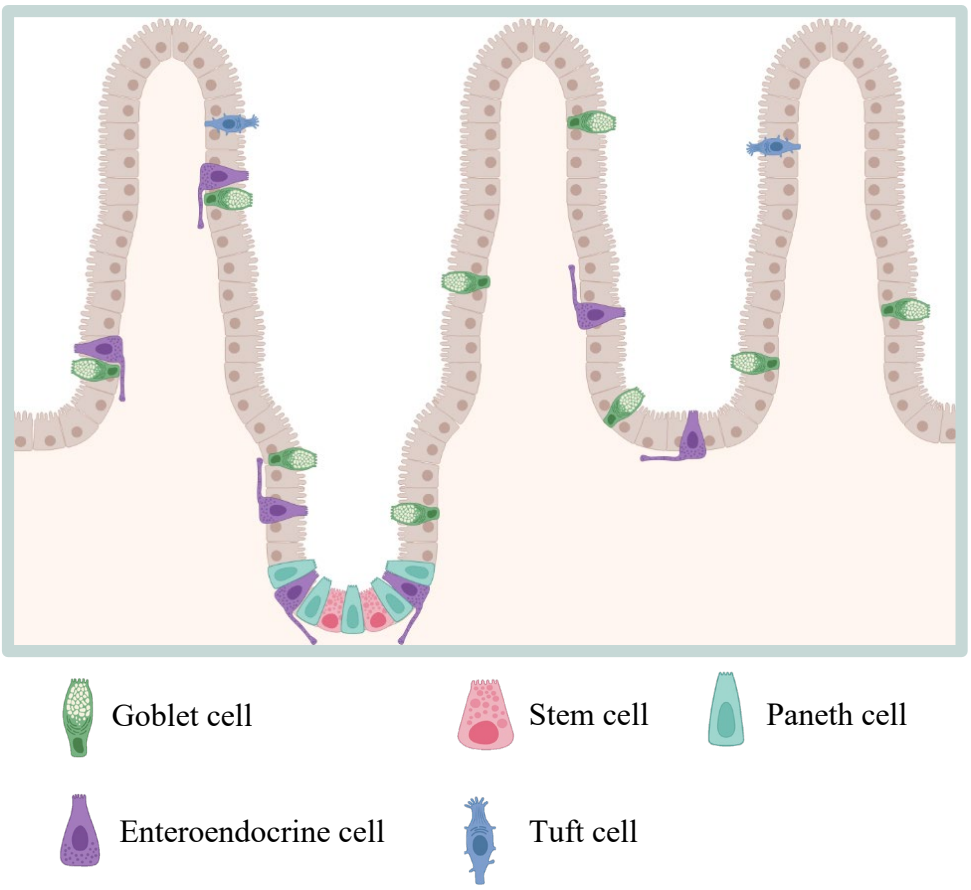

Figure 1: Close-up of the human small intestinal epithelium. Epithelial cells assemble in a crypt-villus structure with microvilli lining individual cells, for maximizing epithelial surface area. A thin, loosely-adherent mucus layer sits atop the epithelium. The gut microbiome and luminal contents sit atop this layer (created with BioRender).

The small intestine is divided into the duodenum, jejunum, and the ileum from top to bottom. These segments are lined with a layer of columnar epithelial cells bound by junctional complexes [2]. The expansive surface area of the small intestine is vital for the digestion and absorption of food, electrolytes, and vitamins. The formation of intestinal epithelial cells into wavy infolding of crypt-villus structures along the small intestine are responsible for this large surface area [3]. These crypt and villus structures are even striated with their own microvilli to further maximize epithelial surface area [4].

There exist a number of different cell types such as enterocytes, Goblet cells, Paneth cells, enteroendocrine cells, and intestinal stem cells. Undifferentiated stem cells that differentiate into these cell types are located within the crypts of the intestinal cell wall. Although each cell type has specific functions, they cooperate to absorb nutrients, form a physical barrier for immune defense, provide separation from the external luminal environment, and form an interface for the communication and preservation of the intestinal microbiome. The intestinal mucosa is formed by the single-cell layer of intestinal epithelial cells, the mucus layer and the intestinal microbiome. The majority of the estimated 100 trillion bacteria in the human gut are commensal anaerobic bacteria [5]. In recent decades, scientists have highlighted the importance of the gut microbiome in immune defense against pathogens as part of the intestinal mucosa [6]. This microbiome helps to characterize the physiological environment and immune responses of the GI tract [5].

2b. The Role of Intestinal Mucus and the Gut Microbiome

However, pathogenic intestinal microbes can trigger bodily immune responses. Thus, the intestinal mucus layer provides a physical barrier that separates intestinal epithelial cells from the intestinal microbiome and serves as a mediator of interaction between human cells and bacteria [7]. In the large intestine and stomach, the intestinal epithelium is covered by a double layer of mucus. The inner layer of mucus is thick and firmly attached to the epithelium, while the outer layer of mucus is thinner and more free-flowing. However, in the small intestine, the epithelium is covered by a single layer of loosely adherent mucus layer [4]. Mucin is the main structural component of mucus in the body and is found in a variety of different forms. Mucins are a class of glycosylated

proteins with oligosaccharide side chains. Through intermolecular interactions, mucins form a gel-like structure that features pores of various sizes (10 – 500 nm) [8]. Mucus and mucin glycoproteins are enriched with anti-microbial peptides (AMPs) and secretory antibodies that provide protection against pathogens. Although there exist 17 types of mucin [9], Goblet cells of the small intestinal epithelium primarily secrete MUC2, which is the predominant gel-forming mucin along the GI tract [10]. MUC5AC, MUC5B, MUC6, MUC7, MUC8, MUC9, and MUC19 are other secretory gel-forming mucins [11]. These mucins are primarily glycosylated by the carbohydrate groups N-acetylgalactosamine (GalNAc), N-acetylglucosamine (GlcNAc), sialic acid (NeuNAc), galactose (Gal), and fucose. These carbohydrates account for 80% of the glycoproteins' weight and contribute to mucins' high molecular weight. The protein backbone, which comprises the remaining 20% of the molecular mass, has distinct regions. Tandem repeats of the amino acids serine, threonine, and proline make up the central glycosylated region where the glycans are attached [12].

Intestinal mucus has a number of biological functions due to its material properties and biochemical composition. Reversible and covalent crosslinking of its mucin glycoproteins allows mucus to form a 3D hydrogel matrix [12]. As a viscoelastic hydrogel, mucus exhibits both viscous and elastic properties as well as shear-thinning and self-healing behavior. Under constant stress, mucus thins and becomes more fluid-like [13]. Because of these characteristics, mucus can continuously shed out of the small intestine while keeping pathogens trapped within the mucus [14]. Mucus is also highly porous with pore sizes in the order of 100 nm [15]. The various pore sizes of mucus allow for the filtering and selective permeability of nutrients, ions, and microbes

[11]. This selective permeability is supplemented by electrostatic interactions and interaction filtering that prevents harmful microbes from reaching epithelial cells [16]. Thus, intestinal mucus serves as a spatial barrier that permits the transport of nutrients into the epithelium that can also concurrently protect the epithelium from pathogens, toxins, and harmful byproducts of digestion [13]. While preventing the penetration of harmful microbes, mucus allows for the spatial organization of commensal microbes within the mucus itself. Due to the 3D matrix gel structure of mucus, microbes can organize into different populations within the mucus. Positions of these microbes can even be optimized such that mucus can form a more effective physical barrier [17]. Intestinal mucus also biochemically interacts with both commensal and pathogenic microbes. Both commensal and pathogenic microbes use mucus as nutrients as well as bind with and lyse mucin through a number of different strategies [18]. Mucin glycans have been demonstrated to selectively bind against harmful microbes to prevent these microbes from multiplying uncontrollably [19]. Dysfunction of the intestinal mucus barrier is associated with the propagation of numerous diseases such as cystic fibrosis, Crohn's disease, and ulcerative colitis [20]. For example, Distal ileal obstruction syndrome can develop in adults with cystic fibrosis, which causes mucus to accumulate at the distal end of the ileum [21]. The disease also prevents the detachment of the N-terminus of the MUC2 protein. This, in conjunction with the cystic fibrosis transmembrane conductance regulator (CFTR) protein dysfunction, causes mucus buildup [22].

2c. Current in vitro Models of the Intestinal Epithelium

Intestinal mucus is undoubtedly key in maintaining the homeostasis of the GI tract and the human body as a whole. Researchers have developed *in vitro* intestinal epithelial models that simulate and advance the understanding of the intestinal epithelium. These models mimic the structure and cell makeup of the intestinal epithelium. Models incorporating mucus as a physical barrier between seeded epithelial cells and microbes have also been created. However, there have been challenges and limitations associated with the creation of mucus layers. A number of different *in vitro* models of the intestinal epithelium have been developed over the years by the David Kaplan laboratory at Tufts University, as well as researchers in other academic institutions. Researchers have used transwell systems, organoids, and scaffolds as platforms for studying the intestinal epithelial system and for growing intestinal epithelial cells *in vitro*.

The common cell lines used intestinal epithelial cell sources in *in vitro* intestinal epithelial studies are Caco-2 and HT-29 cell lines and these exhibit enterocyte properties upon differentiation. These cell lines are derived from human colorectal adenocarcinoma and they have the benefit of being an immortalized cell line that can proliferate indefinitely under the right conditions [23]. Caco-2 and HT-29 cells, as well as Caco-2-HT-29-MTX co-cultures, have often been used in drug permeability and absorption studies [24]. Caco-2 cells are also typically grown on transwell inserts, which are plastic inserts that can be placed within cell culture well plates. At the base of the insert is a permeable membrane and this helps to create a physical separation between the well plate to form a two-chamber system. Transwells have allowed researchers to

investigate cell migration across this permeable membrane [25]. To assess the barrier functions of cells if, for example, microbes and Caco-2 cells were seeded above the transwell membrane, researchers can record Trans-epithelial electrical resistance (TEER), which measures the electrical resistance of the membrane. These immortalized cell lines have limitations, however. Caco-2 cells, for example, are unable to produce a mucus layer upon differentiation, and its differentiation in general is difficult to control [26]. HT-29 cells show impaired glucose metabolism which can lead to glycogen accumulation not seen normally in *in vivo* settings [27].

To address some of these limitations and allow for the more accurate study of intestinal epithelial cells *in vitro*, intestinal organoids (enteroids), have been used. The Kaplan lab has used enteroids in the creation of *in vitro* models to study the intestinal epithelium. The group has incorporated enteroids onto porous 3D silk scaffold platforms, although they have also used this platform before with Caco-2 and HT29-MTX cells. In 2015, the group created an *in vitro* intestinal epithelial model which incorporated porous 3D silk scaffolds, Caco-2 and HT29-MTX cells as epithelial cells, and primary human intestinal myofibroblasts. The cell lines were seeded on the inner surface of a silk scaffold shaped into a hollow cylinder. Human intestinal myofibroblasts were seeded within the scaffold bulk space between the inner and outer surfaces to support the epithelial cell growth. Notably, the model was able to produce mucus layers within the scaffold lumen [28]. In 2017, the group incorporated human small intestinal enteroids (HIEs) into an *in vitro* intestinal epithelial model using the same silk scaffold platform. These enteroids were able to differentiate into enterocytes, Paneth cells, enteroendocrine cells, and mucus-secreting Goblet cells. MUC2 expression was also

found within the model, alluding to the formation of a mucus layer. Although, a physical barrier of mucus was not described in their publication of the results of this model. The team instead reported on the HIEs' ability to mature into four major epithelial cell types and exhibit an anti-bacterial response to *Escherichia coli* (*E.* coli) infection [29]. More recently, in 2022, the Kaplan lab incorporated undifferentiated human intestinal enteroids into an updated porous 3D silk scaffold: a half-scaffold of the previous hollow cylinder scaffold that exposed the inner surface of this scaffold. Here, they demonstrated the formation of two physiologically relevant oxygen gradients that could support the co-culture of epithelial cells with a microbiome, in addition to the formation of a mucus layer [30].

2d. Shortcomings of Current Models

In vitro intestinal epithelial models have demonstrated mucus layer formation from immortalized cell lines and intestinal epithelial organoids. However, mucus layers formed *in vitro* have limitations. Oftentimes, the mucus layer secreted by Caco-2/HT29-MTX co-cultures or human intestinal organoids is insufficient in that there is a low yield of mucus produced from these cells. A thinner mucus layer weakens the biochemical and physical spatial barrier between cultured epithelial cells and microbiome. This insufficiency can cause bacteria overgrowth and limit the duration of study in *in vitro* models [31]. Synthetic mucins have been created to address these issues of low yield. However, these synthetic mucins also have their own set of limitations. No single synthetic mucus has been found that can reproduce all the major biological and material properties of native intestinal mucus. Certain polypeptide backbone polymers, for example, have demonstrated adequate yield and biocompatibility, but fail to form gel-

like structures [32]. Non-peptide polymers have been shown to form a sufficient physical barrier similar to native mucus, however, the biological effects differ from native mucus [33]. Therefore, there is a need to create a synthetic mucin that can be applied to *in vitro* intestinal epithelial models that also addresses the limitations associated with current synthetic and cell-culture-derived sources of mucus.

Caco-2 cells, as opposed to intestinal organoids, were used for all experiments described. Organoids are more biologically relevant in representing the native human intestine compared to Caco-2 cells. Unlike Caco-2 cells, organoids have a 3D morphology more similar to native intestine physiology. Organoids also differentiate into multiple cell types as opposed to just enterocytes with Caco-2 cells. Initial experiments were performed with organoids rather than Caco-2 cells. However, organoids proved more fragile than Caco-2 cells to maintain and significantly more expensive to perform experiments with. Therefore, synthetic mucins were screened with Caco-2 cells.

2e. Silk-derived Synthetic Mucin

In this study, synthetic mucins of silk fibroin and amino sugar composition were screened for their ability to mimic the protective functions of intestinal mucus. These mucins were developed based on a study by Werlang et al. In this study, silk-based glycopolymers were able to prevent *Streptococcus* biofilm formation by reproducing native mucin's ability to neutralize pathogens. Silk fibroin (SF) was used as the glycopolymer backbone for its biocompatibility, stability, and ability to be processed into an aqueous solution [51]. Silk fibroin has a high molecular weight of ~420 kDa [37], similar to that of MUC2 at ~540 kDa [52]. SF also contains glycosylatable amino acids such as serine, threonine, and proline. SF was conjugated with GalNAc since it's a

glycan found in native human mucus [51]. As described in Section 2b, GalNAc is a primary glycan found in the intestinal mucin MUC2. In the study by Werlang et al. SF(S)-GalNAc specifically was able to reduce *S. mutans* biofilm formation by 98% in an *in vitro* oral cavity model [51]. Additionally, synthetic mucins of SF-sugar composition were screened for their potential to mimic the structure of MUC2. Like MUC2, the serine amino acid residues of SF can be glycosylated by galactose derivatives such as GalNAc and GalN.

2f. The Goals of this Study

The immediate goals of this study were to demonstrate that synthetic mucin could act as a physical barrier that could protect intestinal cells from bacteria penetration and also support the co-culture of intestinal cells and gut microbiota. Ultimately, a synthetic mucin fulfilling these goals could not be identified and the results of this study are inconclusive. However, if a suitable synthetic mucin candidate was identified, the next steps would be to confirm compatibility with intestinal organoids and to incorporate the synthetic mucin into the 3D half-scaffold model developed by the Kaplan lab. Overall, the research aimed to create a more comprehensive intestinal model by incorporating synthetic mucin into existing *in vitro* intestinal models. Such research could ultimately advance the understanding of microbiome-intestinal epithelium interactions and of the small intestine generally.

3. Materials and Methods

3a. Caco-2 Cell Culture

Caco-2 cells were grown for approximately 1-2 weeks in a T-75 flask until cells reached 80%-100% confluency. Cells were fed every other day with growth media consisting of 89% DMEM + GlutaMAX, 10% FBS, and 1% Pen strep, and 10 µg/mL of human transferrin. Once cells reached optimal confluence, cells were rinsed with 5 mL of PBS and then digested with Trypsin-EDTA for 10 minutes in a 5% CO_2 incubator at 37 °C. The cells were transferred and evenly dispersed in a vial. 10 µL of cells were aliquoted and mixed with 10 µL of Trypan blue. The remaining cells were centrifuged at 1200 RPM for 5 minutes. The aliquoted cells were counted using a hemocytometer to estimate the total number of cells in the vial.

3b. Caco-2 Transwell Seeding

For experiments, 10,000 cells were seeded for each transwell, so the total number of cells needed for each experiment was calculated based on this constant. After centrifugation, the remaining cell pellet was resuspended in growth media. Extra cells were passaged into another T-75 flask. Cells for experiments were pipetted onto transwell inserts in 24-well plates and these transwells were then fed with growth media: 200 µL on top of the membrane and 500 µL underneath the membrane in the bottom compartment. Cells were seeded onto different plates based on bacteria group. Transwells were used to simulate the intestinal epithelium, with Caco-2 cells seeded on the transwell membrane and culture media being added to the top and bottom chambers. These seeded cells were fed on a MWF (Monday, Wednesday, and Friday)

schedule for 2-3 weeks. These cells were fed until they reached 100% confluence and reached TEER in the range of 500 to 800 Ohms x cm^2. At this point transwells had approximately 20,000 cells. According to literature, TEER between 200 and 1000 Ohms x cm^2 is indicative of good Caco-2 monolayer integrity [34], and TEER between 500 and 800 Ohms x cm^2 has also been shown to indicate good integrity [35]. Thus, TEER values in the range of 200 to 1000 Ohms x cm^2 were considered to have strong Caco-2 monolayer integrity.

3c. Aqueous Silk Fibroin Creation

An aqueous silk solution was created based on a previous protocol developed by the Kaplan laboratory. Bombyx mori silkworm (Tajima Shoji Co. Ltd., Yokohama, Japan) cocoons were cut then degummed by boiling in 0.02 M Na2CO3 solution for approximately 60 minutes. The degummed silk was rinsed with deionized water to remove residual sericin protein. The remaining fibroin protein was dried overnight at room temperature inside a fume hood. The dried fibroin was dissolved in 9.3M LiBr (Sigma-Aldrich, St. Louis, MO) solution at 60 ºC for 4 hours. After the fibroin solution achieved a light brown color, the fibroin was dialyzed against deionized water with 6 water changes across 48 hours. Afterward, the resulting dialyzed fibroin was centrifuged at 9,000 rpm at 4°C for 20 minutes. The concentration of silk fibroin was determined by measuring its weight on a weight boat. A specified volume of aqueous fibroin was allowed to dry on the weight boat and its weight per volume percentage was obtained [54].

3d. SF(S)-GalNAc, SF(S)-GalN, and SF(D, E)-GalNAc Creation

SF(S)-GalNAc Creation

SF(S)-COOH and SF(S)-EDA were synthesized as prerequisites for the creation of SF(S)-GalNAc. For the synthesis of SF(S)-COOH, “aqueous SF solution was carboxylated in a nucleophilic substitution reaction in a highly alkaline reaction environment, in the presence of chloroacetic acid (Sigma-Aldrich, St. Louis, MO) at pH ~13.5” [37]. SF(S)-COOH was then used to synthesize SF(S)-EDA. For the synthesis of SF(S)-EDA, “The carboxylated SF (SF(S)-COOH) was covalently conjugated with primary amines of ethylene diamine (EDA) hydrochloride (Sigma-Aldrich, St. Louis, MO) by carbodiimide coupling in the presence of N-3-Dimethyl amino propyl-N’-ethyl arbodiimide (EDC) hydrochloride, and N-Hydroxy Succinimide (NHS) (Sigma-Aldrich, St. Louis, MO)” [37]. Lastly, SF(S)-EDA was used to synthesize SF(S)-GalNAc. For the synthesis of SF(S)-GalNAc, “The aminated SF solution (SF(S)-EDA) were conjugated with carboxylic acid moieties of 4-carboxybutyl N-acetyl-β-D-galactosaminide (β-GalNAc-Bu-COOH) (Sussex Research, Ottawa, Canada) …” [37].

SF(S)-GalN Creation

SF(S)-COOH was synthesized as a prerequisite for the creation of SF(S)-GalN. For the synthesis of SF(S)-GalN, “SF(S)-COOH was conjugated with amines of D (+)-Glucosamine Hydrochloride (Sigma-Aldrich, St. Louis, MO) by carbodiimide coupling in the presence of EDC and NHS (Sigma-Aldrich, St. Louis, MO) …” [37].

SF(D, E)-GalNAc Creation

SF(D, E)-EDA was synthesized as a prerequisite for the creation of SF(D, E)-GalNAc. For the synthesis of SF(D, E)-EDA, aqueous SF solution was “covalently conjugated with primary amines of ethylene diamine (EDA) hydrochloride (Sigma-Aldrich, St. Louis, MO) by carbodiimide coupling in the presence of EDC, and NHS (Sigma-Aldrich, St. Louis, MO)” [37]. For the synthesis of SF(D, E)-GalNAc, “The aminated SF solution (SF (D, E)-EDA) were conjugated with carboxylic acid moieties of 4-carboxybutyl N-acetyl-β-D-galactosaminide (β-GalNAc-Bu-COOH) (Sussex Research, Ottawa, Canada) by carbodiimide coupling in presence of EDC and NHS (Sigma-Aldrich, St. Louis, MO)” [37].

3e. TEER Measurements

After cells reached 100% confluence, TEER measurements were taken each day. TEER was used to assess the strength of Caco-2 monolayers in the presence of varying synthetic mucin and bacteria conditions. TEER measurements were concluded 24-48 hours’ post-bacteria application. With a TEER probe, measurements were taken for every transwell. Before taking measurements, the probe was submerged in 70% ethanol for at least 10 minutes for sterilization. The probe was then submerged in Caco-2 growth media for 2 minutes for acclimation. The short electrode of the TEER probe was placed within the transwell insert and the long electrode of the TEER probe was placed underneath the insert into the well underneath. The short electrode was made sure to not make direct contact with the Caco-2 cells and transwell membrane. The TEER probe was designed in such a way that if inserted correctly, the short electrode would not make contact with the permeable membrane while the long electrode would

make contact with the surface of the well underneath. TEER measurements, in Ohms x cm^2, were read from a Volt/Ohm meter. For accurate measuring, the probe was placed in each transwell for at least 3 seconds. On days when synthetic mucin or bacteria were applied to the transwells, TEER measurements were taken immediately beforehand.

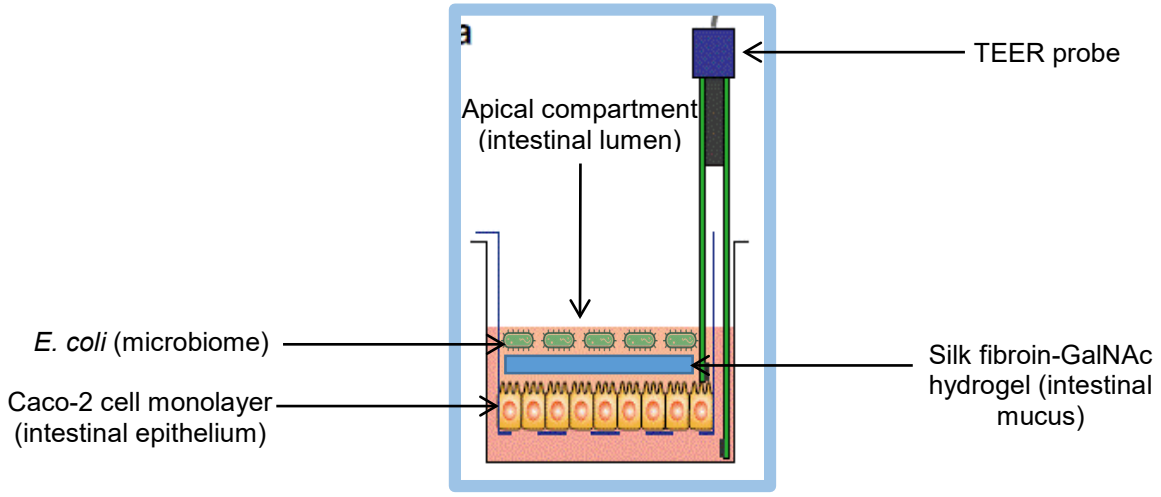

Figure 2: Setup for taking TEER (transepithelial electrical resistance) measurements [57]. The parts of the human body that each component of the transwell represents is shown in parentheses ( ).

3f. Synthetic Mucin Application

Synthetic mucin was applied once Caco-2 cells were deemed to have formed sufficient monolayers atop transwells. In the first 5 experiments, this judgement was made based on observation of transwells under a lab benchtop compound microscope. Caco-2 monolayers were deemed adequately dense if they were 100% confluent. However, this assessment was changed for the final 2 experiments. In order to eliminate inconsistencies in experimental data, sufficient monolayer formation was assessed primarily on TEER measurements made at least 1 week prior to synthetic mucin application. In the time between when cells were seeded onto transwells and when synthetic mucin was applied, TEER was expected to increase until reaching a

“plateau”. At this plateau, TEER would maintain a maximum TEER value for 3-5 days before decreasing rapidly. For these later experiments, synthetic mucin was applied at the start of this TEER plateau, and this was determined based on measuring TEER across multiple days.

In preparation for synthetic mucin application, antibiotic-free Caco-2 growth media was created. This antibiotic-free media was created with the same components as normal Caco-2 media, but without Pen strep. This media was used to feed cells during experiments and to dilute synthetic mucins and bacteria. Undiluted synthetic mucin materials were UV-treated under a biosafety hood for 30 minutes for disinfection, prior to synthetic mucin creation. Synthetic mucin materials were prepared before the start of experiments and came either in solid or aqueous form. The mass of synthetic mucin material needed to create a synthetic mucin solution was determined by using the percent concentration of solution specified for the experiment and the volume of synthetic mucin solution needed to fill all transwells of a mucin group. Synthetic mucin materials were weighed, then mixed and diluted in antibiotic-free Caco-2 media. Transwells were filled with 200 µL of solution each. Synthetic mucin was only applied to the apical compartment of transwells.

3g. Bacteria Culture and Application

E. coli Nissle 1917 (EcN) bacteria and Adherent-invasive *E. coli* bacteria were used as the “Commensal” and “Pathogenic” strains respectively for experiments. Both bacteria strains were stored at -80 °C in cryovials. For each cryovial, a small dab of bacteria was scraped from the cryovial using a 10-µL pipette tip and then resuspended in 2 mL of LB media. The bacteria were mixed within the LB media with a pipette,

sealed, and then incubated in a shaking incubator. The bacteria were incubated at 37 °C at 80 x *g* for a minimum of 4 hours. After incubation, 1 mL of each bacteria/LB media mixture was added to 2 different cuvettes and 1 mL of only LB media was added to a third cuvette. The cuvette containing only LB media was used as a blank to calibrate a spectrophotometer. The spectrophotometer measured the absorbance of each cuvette and this value was used to calculate bacteria concentration. Bacteria was seeded at an MOI of 0.1 (2,000 bacteria for 20,000 Caco-2 cells). 50 µL of bacteria was pipetted onto each transwell. These metrics were used to determine how to isolate 2,000 bacteria for each transwell. Bacteria were then applied atop the synthetic mucin that was applied a 1-2 days before. Bacteria was never applied to the “Control” plate.

3h. Immunostaining

Caco-2 cells have a heterogeneous morphology meaning the shape of cells can be different from one another [38]. However, Caco-2 cells normally have defined borders between each other which are formed by tight junctions [39]. These tight junctions possess a stainable antibody-known as ZO-1. Using ZO-1 Monoclonal Antibody, ZO-1 antibodies in tight junctions could be visualized using confocal microscopy [62]. Additionally, DAPI fluorescent dye was used to stain and help visualize cell nuclei [53].

Fixation

Caco-2 seeded transwells were fixed in preparation for fluorescence imaging and SEM (scanning electron microscope) imaging. Caco-2 cells were fixed 1-2 days after bacteria application. For Experiments 5, 6, and 7, half of replicates were fixed 24 hours’

post-bacteria application and the other half of replicates were fixed 48 hours' post-bacteria application. Media was aspirated from the top and bottom compartments of each well prior to fixation. 200 µL of 4% PFA (paraformaldehyde) was pipetted into the top compartment and 500 µL of 4% PFA was pipetted into the bottom compartment. The cells were left in PFA for 10 minutes at room temperature. PFA fixation was performed under a fume hood rather than a biosafety cabinet since PFA can be toxic. The PFA was then aspirated from the transwells and the transwells were rinsed 3 times with equivalent volumes of PBS (Phosphate-buffered saline), waiting a couple of minutes between rinses. At this stage, cells could be left submerged in PBS at 4 °C for up to 1 week. However, the remaining immunostaining procedures were usually performed either immediately or at most a couple days after fixation.

Permeabilization, Blocking, and Antibody Staining

After fixation, Caco-2 transwells were prepared for fluorescence imaging through permeabilization, blocking, and antibody staining. For all experiments except for Experiment 7, transwell membranes were removed from the transwell inserts using a sharp tweezer. These membranes were carefully arranged in 96-well plates with the side of transwell containing cells facing up. For Experiment 7, however, transwell membranes were not removed from the transwell inserts and the following immunostaining steps were performed for the original 24-well transwell plates. A blocking solution of 0.25% Triton X-100 and 1% BSA diluted in PBS was then prepared. The PBS from the previous fixation step was aspirated from the transwells as well. 200 µL of the blocking solution was pipetted onto each transwell membrane and they were incubated for 10 minutes at room temperature. The solution was then carefully aspirated

using a micropipette to minimize injury to the Caco-2 cell monolayers. 200 µL of the 5% BSA diluted in PBS was pipetted onto each transwell membrane and they were incubated for 30 minutes at room temperature.

During this incubation period 0.5% BSA diluted in PBS was prepared. In this 0.5% BSA solution, ZO-1 Monoclonal Antibody was diluted 1:100. 50 µL of the BSA/ZO-1 solution was pipetted onto each transwell membrane. The 96-well plate(s) of transwell membranes was then wrapped in tin foil to prevent light exposure and left to incubate overnight at 4 °C.

The following day, the BSA/ZO-1 solution was aspirated and the transwell membranes were carefully rinsed with PBS using a micropipette 3 times. In a space with limited light exposure, a 1:1 solution of 0.5% BSA and 1:1000 DAPI was created by diluting in PBS. PBS from the previous step was carefully aspirated and then 50 µL of the BSA/DAPI solution was pipetted onto each transwell. The 96-well plate(s) of transwell membranes were wrapped in tin foil to limit light exposure and incubated for 45-60 minutes at room temperature. Afterwards, this BSA/DAPI solution was carefully aspirated and the transwells were again rinsed with PBS 3 times. At this point, the cells were stored at 0 °C and could be stored for up to several weeks until confocal imaging.

3i. SEM Preparation

For Experiments 1,2, and 4, Caco-2 transwells underwent preparation for scanning electron microscopy (SEM). In these experiments, half of replicates underwent SEM preparation while the rest were immunostained for confocal imaging.

Fixation

Transwells were first rinsed with PBS 3 times., the PBS was aspirated from the transwells. A mixture of 9:1 PBS to 2.5% GA (glutaraldehyde) was mixed with 2.5% GA to create the fixative mixture. 500 µL of this fixative mixture was pipetted onto each transwell insert. The transwells were left to incubate for 60 minutes at room temperature. After the 60-minute incubation period, the fixative mixture was aspirated from the transwells. At this point, the transwells were removed from their 24-well plate inserts using sharp tweezers and transferred to a 96-well plate. The transwells were once again rinsed with 500 µL of PBS 3 times with 2 minutes separating each rinse. The transwells were then stored with PBS at 4 °C. The transwells could be stored in this manner for up to a week, however, the dehydration step was usually performed the following day.

Dehydration

The PBS from the previous step was first aspirated carefully from the transwells. The transwells were rinsed with 500 µL of ultrapure water 2 times with 2 minutes separating each rinse. The transwells were kept at room temperature between these rinses. The transwells were then rinsed with 500 µL of ultrapure water 3 times with 2 minutes separating each rinse. The transwells were placed in a refrigerator at 4 °C between these rinses. Next, 5 solutions of ethanol (EtOH)/ultrapure water with varying concentrations were prepared. Solution of the following concentrations were prepared: 25% EtOH, 50% EtOH, 75% EtOH, 95% EtOH, and 100% EtOH. For each ethanol dehydration, 200 µL of the solution was pipetted into the top compartment and 500 µL of the solution was pipetted into the bottom compartment. With each dehydration, the

previous ethanol solution would be aspirated from the transwells. 25% EtOH was pipetted onto transwells and the transwells were then left in the refrigerator at 0 °C for 10 minutes. Next, 50% EtOH was pipetted onto transwells and the transwells were then left in the refrigerator at 0 °C for 10 minutes. Next, 75% EtOH was pipetted onto transwells and the transwells were then left in the freezer at -20 °C for 15 minutes. Next, 95% EtOH was pipetted onto transwells and the transwells were then left in the freezer at -20 °C for 15 minutes. Next, 100% EtOH was pipetted onto transwells and the transwells were then left in the freezer at -20 °C for 15 minutes. This 100% EtOH dehydration step was performed 2 more times, with the transwells being left in the freezer at -20 °C for 15 minutes between dehydrations. Lastly, the samples were stored in 100% EtOH solution at -20 °C until SEM imaging.

3j. Statistical Analysis of TEER Measurements

Data points represented mean TEER across multiple samples of Caco-2 transwells within each mucin group. Error bars represented standard deviation. For each mucin group, Tukey's multiple comparison test for two-way ANOVA was used to compare means across days. For each day, Dunnett's multiple comparison test for two-way ANOVA was used to compare mucin group means with "No mucin" group means.

4. Results

4a. Experiment 1: Initial Caco-2 Experiment

In this initial experiment, 3 different mucin conditions were tested against 3 different bacteria conditions. The 3 mucin conditions were: “No mucin”, “0.5% SF(S)-GalNAc”, and “1.2% SF + 0.8% SF(S)-GalNAc”. The 3 bacteria conditions were: “Control (No bacteria)”, “Commensal”, and “Pathogenic. 3 replicates were used for each mucin group within each bacteria group. Synthetic mucin was applied immediately after Day 17 measurements and bacteria was applied immediately after Day 18 measurements. TEER for all bacteria sets and mucin groups decreased, following the introduction of synthetic mucin, from Day 17 to Day 19. For “Control” mucin groups, TEER increased after Day 19. Additionally, no statistical differences were found when comparing “No mucin” with the other two mucin groups respectively at all days. For the “Commensal” and “Pathogenic” “0.5% SF(S)-GalNAc” and “1.2% SF + 0.8% SF(S)-GalNAc” mucin groups, TEER increased significantly from Day 19 to Day 20. However, TEER decreased for the “No mucin” groups of these bacteria sets over the same period. For all bacteria sets, following the introduction of synthetic mucin, Day 18 TEER was expected to match or exceed Day 17 TEER. Instead, TEER decreased for all mucin groups from Day 17 to Day 18 and this decrease was statistically significant for Commensal-1.2% SF + 0.8% SF(S)-GalNAc, Pathogenic-No mucin, and Pathogenic-1.2% SF + 0.8% SF(S)-GalNAc groups. In the “Pathogenic” set, “0.5% SF(S)-GalNAc” and “1.2% SF + 0.8% SF(S)-GalNAc” TEERs were significantly greater than the “No mucin” TEER from Day 19 to Day 20. However, no differences were found among “Commensal” mucin groups on Day 20. These results may demonstrate that at least in

the presence of pathogenic bacteria, synthetic mucin helped prevent Caco-2 monolayer degradation (Figure 3).

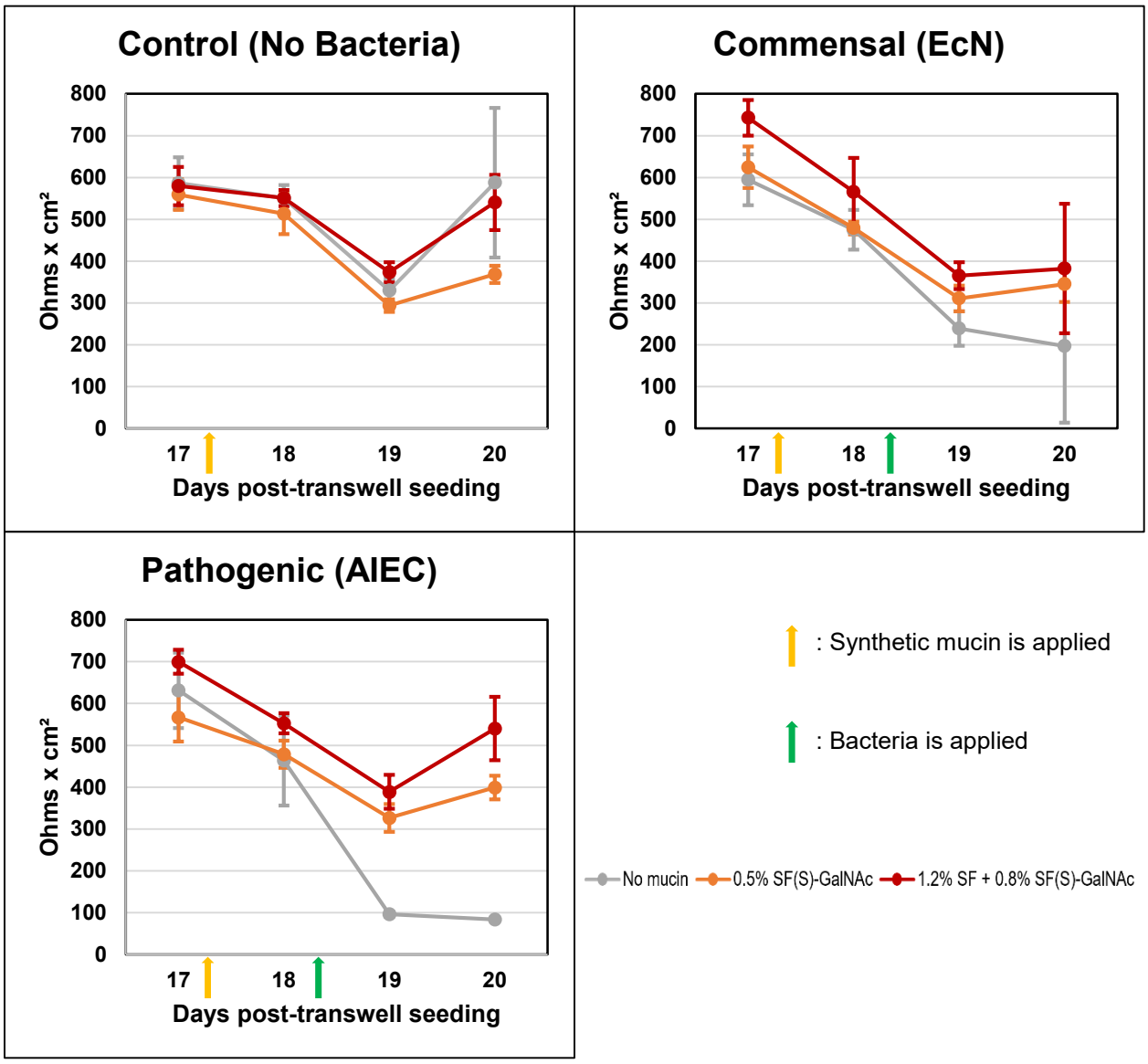

Figure 3: TEER Measurements taken of Caco-2 cells in transwells. Caco-2 transwells were separated into 3 bacteria groups: control (no bacteria), commensal bacteria (EcN), and pathogenic bacteria (AIEC). Caco-2 transwells were also divided into 3 separate mucin groups: No mucin, 0.5% SF(S)-GalNAc, 1.2% silk fibroin (SF) + 0.8% SF(S)-GalNAc. Synthetic mucin was applied 17 days post-transwell seeding. Bacteria was applied 18 days post-transwell seeding. Control-0.5% GalNAc TEER decreased significantly from Day 17 to Day 20, while other "Control" mucin groups remained stable (no significant differences).

TEER for all “Commensal” groups decreased significantly from Day 17 to Day 19, but remained stable afterward. TEER for all “Pathogenic” groups decreased significantly from Day 17 to Day 19, but rebounded for Pathogenic-0.5% SF(S)-GalNAc and -1.2% SF + 0.8% SF(S)-GalNAc.

Following TEER measurements, half of samples were prepared for confocal imaging and the other half for SEM imaging. All “Control” mucin samples exhibited strong ZO-1 and DAPI expression. In these samples, ZO-1 formed a “chicken-wire” pattern around the cells. These traits indicate that monolayer integrity was maintained, even with the addition of a synthetic mucin layer. This chicken-wire pattern, however, could not be identified in the “Commensal” and “Pathogenic” “No mucin” samples. Additionally, in these samples, the lack of ZO-1 indicated that the Caco-2 monolayers degraded. All “0.5% SF(S)-GalNAc” mucin groups did exhibit ZO-1 expression, however, a clear chicken-wire pattern was not identified in the “Commensal” and “Pathogenic” samples which could have indicated Caco-2 monolayer degradation. The same conclusion was drawn for the Commensal-1.2% SF + 0.8% SF(S)-GalNAc and Pathogenic-1.2% SF + 0.8% SF(S)-GalNAc samples (Figure 4).

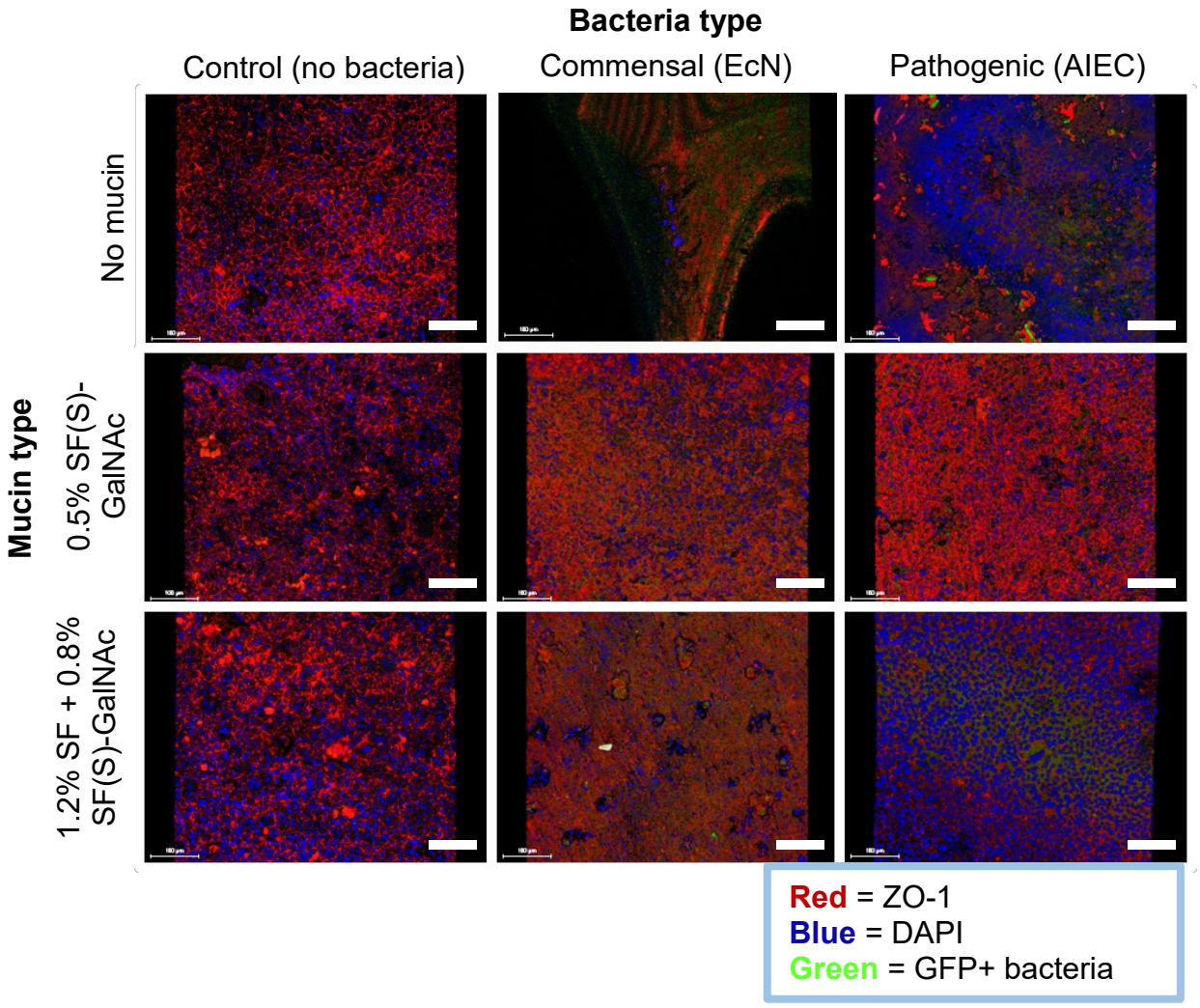

Figure 4: Confocal images taken of Caco-2 cells. Images were taken at 20x magnification. Caco-2 transwells were separated into 3 bacteria groups: control (no bacteria), commensal bacteria (EcN), and pathogenic bacteria (AIEC). Caco-2 transwells were also divided into 3 separate mucin groups: No mucin, 0.5% SF(S)-GalNAc, 1.2% silk fibroin (SF) + 0.8% SF(S)-GalNAc. All "Control" samples exhibited strong Caco-2 monolayer integrity. "Commensal" and "Pathogenic" samples exhibited compromised Caco-2 monolayer integrity. Scale bar = 100 μm

SEM imaging allowed for the visualization of the surface characteristics of the samples. Unlike in confocal imaging preparation, the synthetic mucin layer can be maintained in SEM preparation. Thus, the synthetic mucin layer is somewhat visible in

samples, such as in the Commensal-0.5% SF(S)-GalNAc and Commensal-1.2% SF + 0.8% SF(S)-GalNAc samples. The Caco-2 monolayer was also visible in “Control” samples, however it was difficult to identify the brush-border organization of microvilli typically seen in monolayers [36]. In “Commensal” and especially in the “Pathogenic” samples, bacteria atop the monolayer was visible (Figure 5).

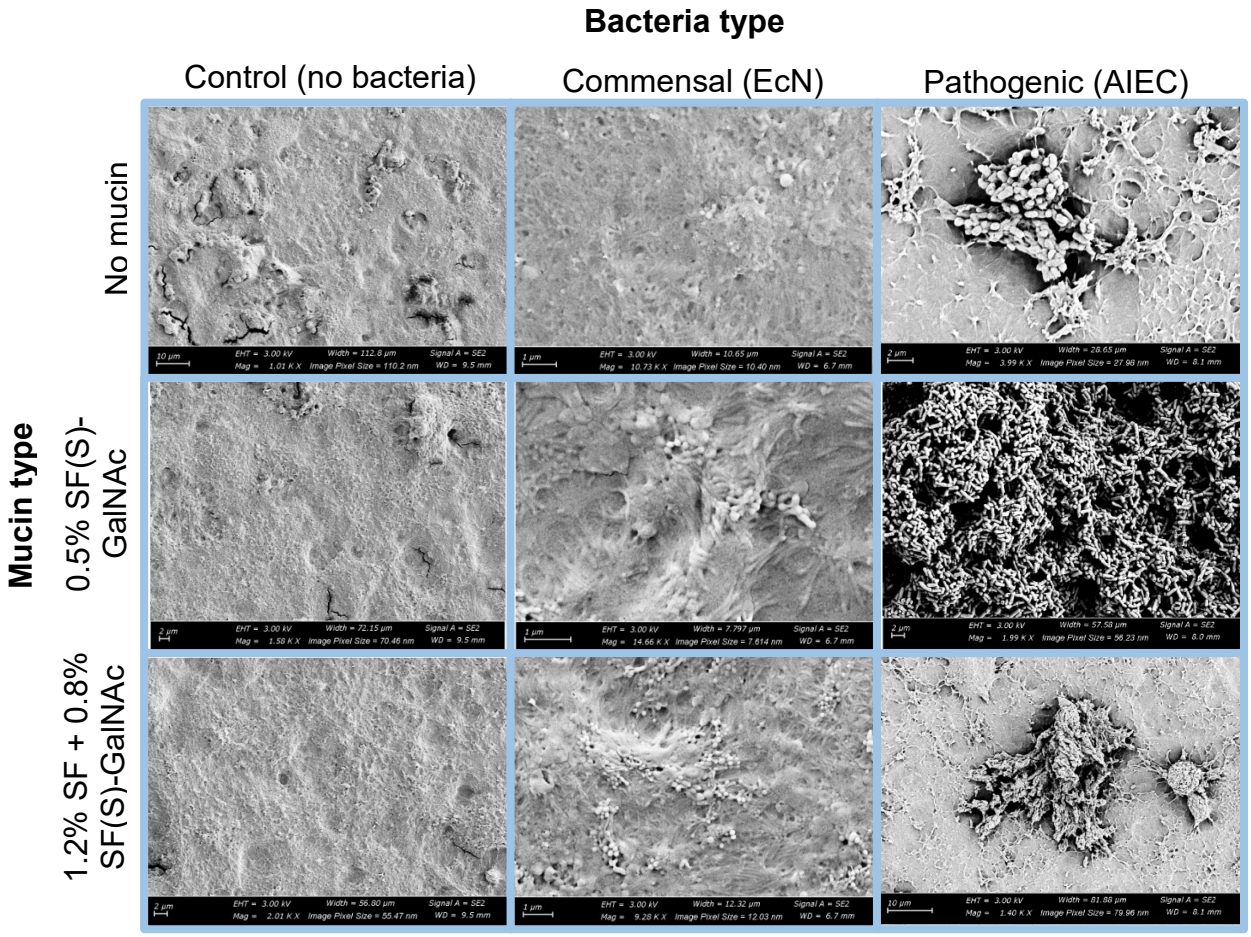

Figure 5: Scanning electron microscope (SEM) images of Caco-2 cells. Caco-2 transwells were separated into 3 bacteria groups: control (no bacteria), commensal bacteria (EcN), and pathogenic bacteria (AIEC). Caco-2 transwells were also divided into 3 separate mucin groups: No mucin, 0.5% SF(S)-GalNAc, 1.2% silk fibroin (SF) + 0.8% SF(S)-GalNAc. Caco-2 monolayers were visible across “Control” samples. Caco-2 monolayers were also somewhat visible in “Commensal” samples, underneath visible mucin layers in the Commensal-0.5% SF(S)-GalNAc and -1.2% SF + 0.8% SF(S)-GalNAc groups.

Bacteria infiltration was visible in “Pathogenic” samples. Scale bar of “2 μm” – “10 μm” is on bottom left of each image.

Results Summary (Experiment 1)

In the “Control” set, “No mucin” and “1.2% SF + 0.8% SF(S)-GalNAc” TEER was stable from Day 17 to Day 20 while “0.5% SF(S)-GalNAc” TEER decreased significantly over the same period. In the “Commensal” set, TEER for all mucin groups decreased significantly post-mucin application, but stayed level post-bacteria application. In the “Pathogenic” set, TEER for all mucin groups decreased significantly post-mucin and post-bacteria application. However, “0.5% SF(S)-GalNAc” and “1.2% SF + 0.8% SF(S)-GalNAc” TEER rebounded and significantly increased from Day 19 to Day 20. In the “Pathogenic” set, the difference in TEER between “No mucin” and other mucin groups may have suggested that synthetic mucins helped preserve Caco-2 monolayer integrity in the presence of pathogenic bacteria. “Control” TEER data supported confocal data which exhibited that Caco-2 monolayer integrity was maintained for all samples and that cells could tolerate synthetic mucin presence. However, “Commensal” and “Pathogenic” TEER data did not support confocal data, which exhibited that samples had compromised Caco-2 monolayer integrity.

4b. Experiment 2: Comparing Silk Fibroin with Sugar-Conjugated Silk Fibroin

The previous experiment was repeated with slight modification: 2% SF was tested rather than 0.5% SF(S)-GalNAc. 5 replicates were used for each mucin group within each bacteria group. Synthetic mucin was applied immediately after Day 20 measurements and bacteria was applied immediately after Day 22 measurements. In the “Control” set, no significant change in TEER was observed between Day 20 and

Day 24 for the “No mucin” and “2% SF” mucin groups. However, a significant decrease in TEER was observed for the “1.2% SF + 0.8% SF(S)-GalNAc” group across these days. In the “Commensal” set, there was no significant difference in TEER between “No mucin” and the other mucin groups at all days. From Day 20 to Day 21, “No mucin” TEER significantly decreased, however, there was no significant difference in “No mucin” TEER from Day 21 to Day 24. Compared to Day 20, TEER was significantly lower following bacteria introduction for all “Commensal” mucin groups. Additionally, there were no significant differences in TEER between “Commensal” mucin groups following bacteria introduction. In the “Pathogenic” set, there was no significant difference in TEER from Day 20 to Day 22 for all mucin groups. However, there was a very significant decrease in TEER for all mucin groups, following bacteria introduction. No significant differences in TEER were observed between mucin groups following bacteria introduction (Figure 6).

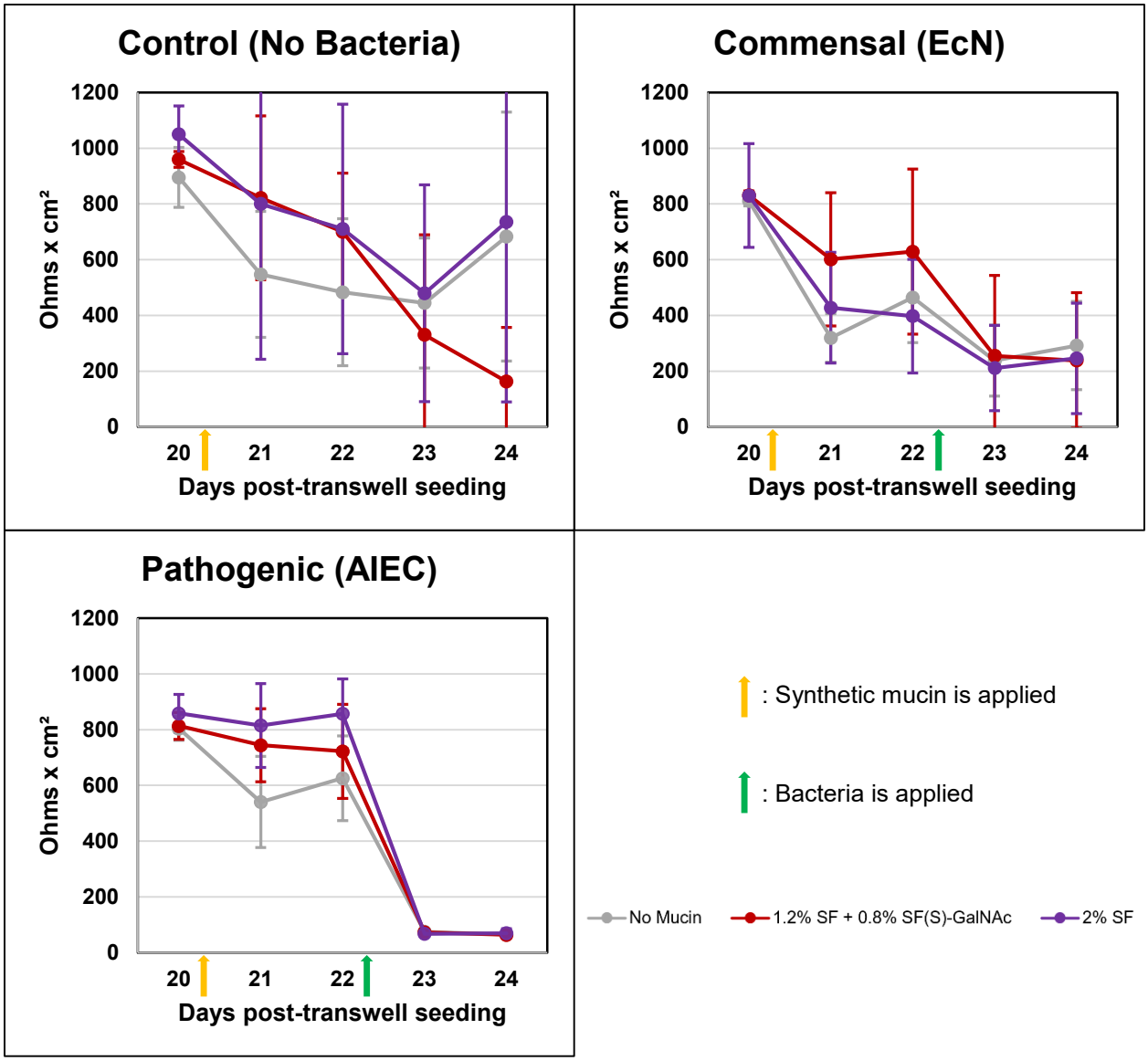

Figure 6: TEER Measurements taken of Caco-2 cells in transwells. Caco-2 transwells were separated into 3 bacteria groups: No bacteria, commensal bacteria (EcN), and pathogenic bacteria (AIEC). Caco-2 transwells were also divided into 3 separate mucin groups: No mucin, 1.2% SF + 0.8% SF(S)-GalNAc, and 2% SF. Synthetic mucin was applied 20 days post-transwell seeding. Bacteria was applied 22 days post-transwell seeding. In the "Control" set, only Control-1.2% SF + 0.8% SF(S)-GalNAc TEER decreased significantly from Day 20 to Day 24. TEER for all "Commensal" and "Pathogenic" groups decreased significantly from Day 20 to 24, although TEER for "Commensal" groups remained above 200 Ohms x cm^2.

Following TEER measurements, half of samples were prepared for confocal imaging and the other half for SEM imaging. Strong ZO-1 expression was visible in the Control-no mucin and Commensal-2% SF samples where a clear chicken-wire between cells was visible. ZO-1 expression was weaker for the remaining “Control” and “Commensal” samples, however chicken-wire patterns were still visible. Few cells were visible in “Pathogenic” samples. Most likely, bacteria in these samples destroyed the Caco-2 monolayer by dislodging cells from their transwell membranes (Figure 7).

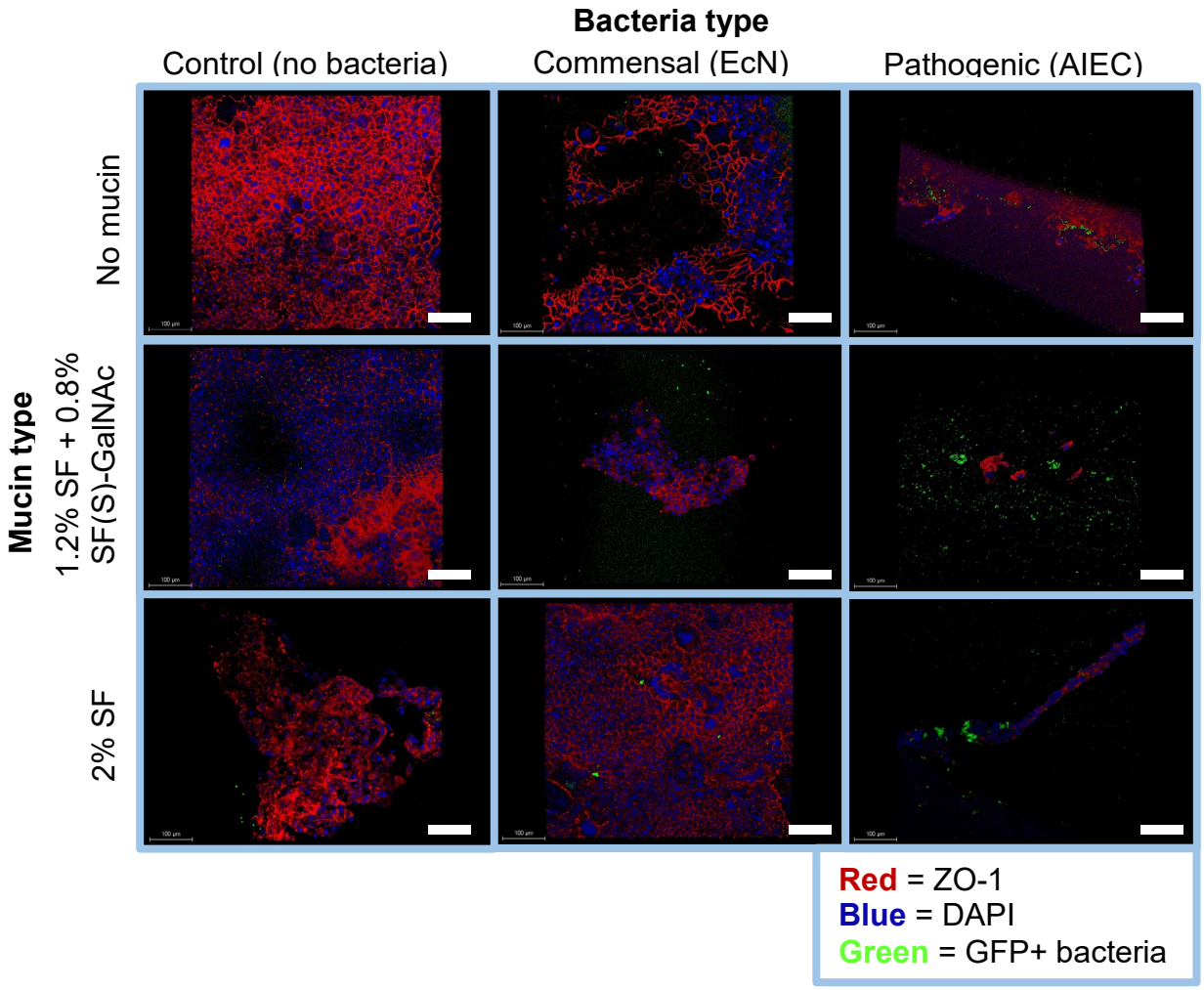

Figure 7: Confocal images taken of Caco-2 cells. Images were taken at 20x magnification. Caco-2 transwells were separated into 3 bacteria groups: No bacteria, commensal bacteria (EcN), and

pathogenic bacteria (AIEC). Caco-2 transwells were also divided into 3 separate mucin groups: No mucin, 1.2% SF + 0.8% SF(S)-GalNAc, and 2% SF. Decent Caco-2 monolayer preservation was observed in all "Control" samples except Control-2% SF. In the "Commensal" set, at least decent monolayer integrity was observed in Commensal-No mucin and -2% SF. Monolayer compromise was clear across all "Pathogenic" samples. Scale bar at the bottom left of each image reads "100 μm".

Clear Caco-2 monolayers were identifiable only in the Control-No mucin and Control-2% SF samples. A faint pattern resembling a Caco-2 monolayer was visible in part of the Commensal-2 SF% sample, however, whether these were healthy Caco-2 cells was unclear. Otherwise, no monolayers were identified in all other samples, indicating that Caco-2 cells were dislodged from the transwell membranes. Interestingly, bacteria were sparsely present on these samples as well. In these samples, rinsing during SEM preparation could have caused both Caco-2 cells and bacteria to dislodge from transwell membranes (Figure 8).

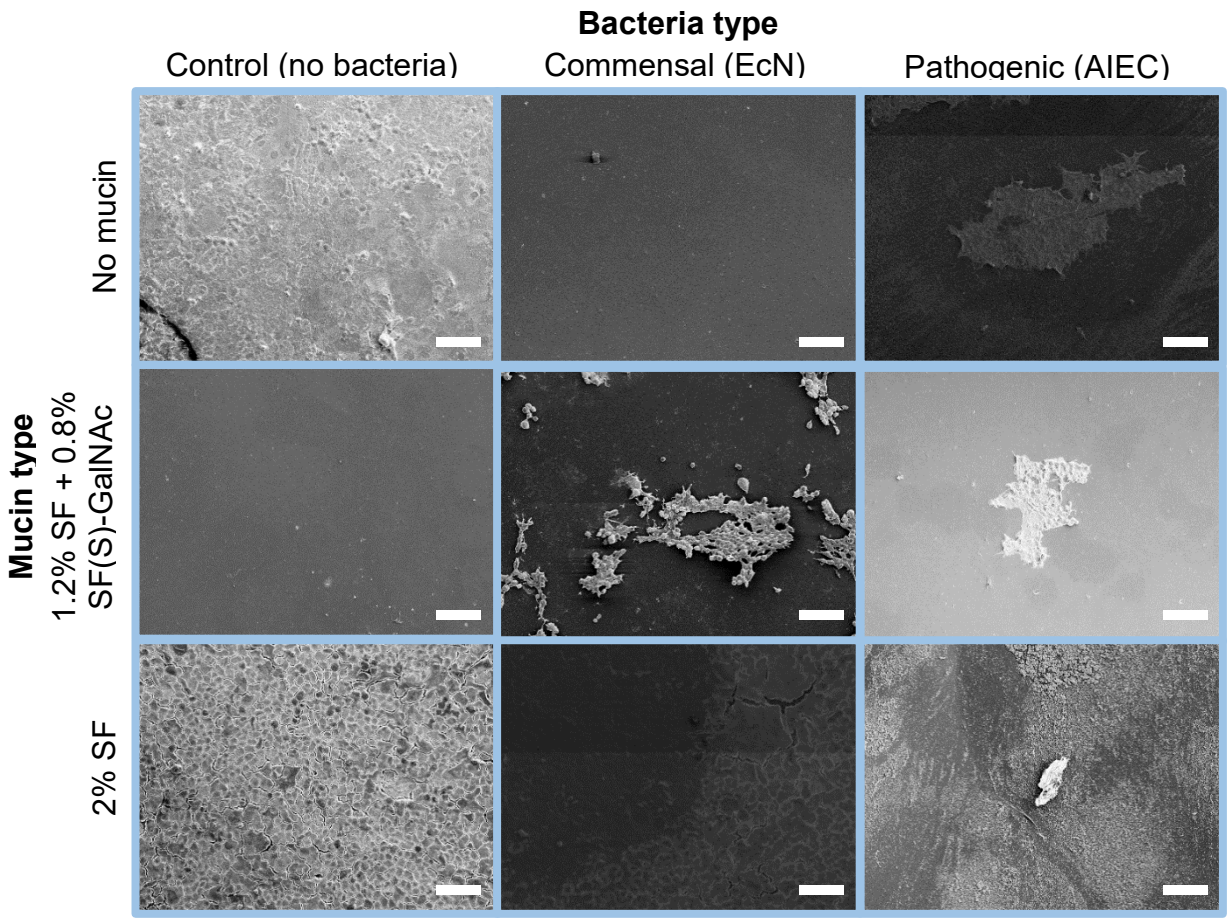

Figure 8: Scanning electron microscope (SEM) images of Caco-2 cells. Images were taken at 100x magnification. Caco-2 transwells were separated into 3 bacteria groups: No bacteria, commensal bacteria (EcN), and pathogenic bacteria (AIEC). Caco-2 transwells were also divided into 3 separate mucin groups: No mucin, 1.2% SF + 0.8% SF(S)-GalNAc, and 2% SF. Among all SEM samples, Caco-2 monolayers were clearly visible in only the Control-No mucin and Control-2% SF samples. Scale bar = 100 µm

Results Summary (Experiment 2)

In the “Control” set, no significant differences in TEER were found for “No mucin” and “2% SF” groups following mucin application, however “1.2% SF + 0.8% SF(S)-GalNAc” TEER significantly decreased. “Control” confocal and SEM samples exhibited decent chicken-wire patterns with the exception of the “1.2% SF + 0.8% SF(S)-GalNAc”

SEM sample which contained no cells and the “2% SF” confocal sample which contained a damaged monolayer. In the “Commensal” set, TEER for all mucin groups significantly decreased from Day 20 to Day 24, however TEER stayed above 200 Ohms x cm^2, which is the minimum TEER associated with strong Caco-2 monolayer integrity [34]. Among confocal samples, however, strong monolayer integrity was only visible for the Commensal-2% SF confocal sample. In the “Pathogenic” set, TEER for all mucin groups decreased significantly and sharply following bacteria application, dropping below 200 Ohms x cm^2. This TEER data was supported by “Pathogenic” confocal and SEM samples which exhibited no monolayer formation.

4c. Experiment 3: Incorporating the Gut Microbiome

The previous experiment was repeated with one change: a human stool sample was added as a bacteria set to represent the human gut microbiome. The gut microbiome was intended to include both commensal and pathogenic bacteria. 5 replicates were used for each mucin group within each bacteria group. Synthetic mucin was applied immediately after Day 21 measurements and bacteria was applied immediately after Day 22 measurements. Average initial TEER was noticeably higher for samples in this experiment compared to the previous two experiments: ~750-1500 Ω x cm^2 vs ~550-1100 Ω x cm^2. In the "Control” set, “No mucin” TEER was consistent until Day 24 when TEER dropped. Following synthetic mucin application, “1.2% SF + 0.8% SF(S)-GalNAc” TEER significantly decreased from Day 20 to Day 24 while “2% SF” peaked at Day 23 then decreased afterward. However, “2% SF” TEER between different days was not significantly different. By Day 24, “1.2% SF + 0.8% SF(S)-GalNAc” TEER was significantly lower than “No mucin” TEER. In the “Commensal” set,

at all days, no significant differences were observed between “No mucin” and the other mucin groups. From Day 21 to Day 24, no significant differences in TEER for “No mucin” and “2% SF” were observed, however, TEER for “1.2% SF + 0.8% SF(S)-GalNAc” decreased significantly over this period. These trends from Day 21 to Day 24 were observed in the “Pathogenic” and “Stool” sets as well. In the “Pathogenic” set, no significant differences were observed between mucin groups on Day 21 and 22. For the “Stool” set, no significant differences were observed between mucin groups across all days, except between “No mucin” and “1.2% SF + 0.8% SF(S)-GalNAc” on Day 24. In all bacteria sets, “1.2% SF + 0.8% SF(S)-GalNAc” TEER decreased from Day 21 to 24, even between Day 21 and 22 when synthetic mucin was applied. Interestingly, “No mucin” TEER was stable in sets containing bacteria, but was not stable in the “Control” set. Lastly, significant differences in TEER were not observed between “No mucin” and “2% SF” for all bacteria sets across all days (Figure 9).

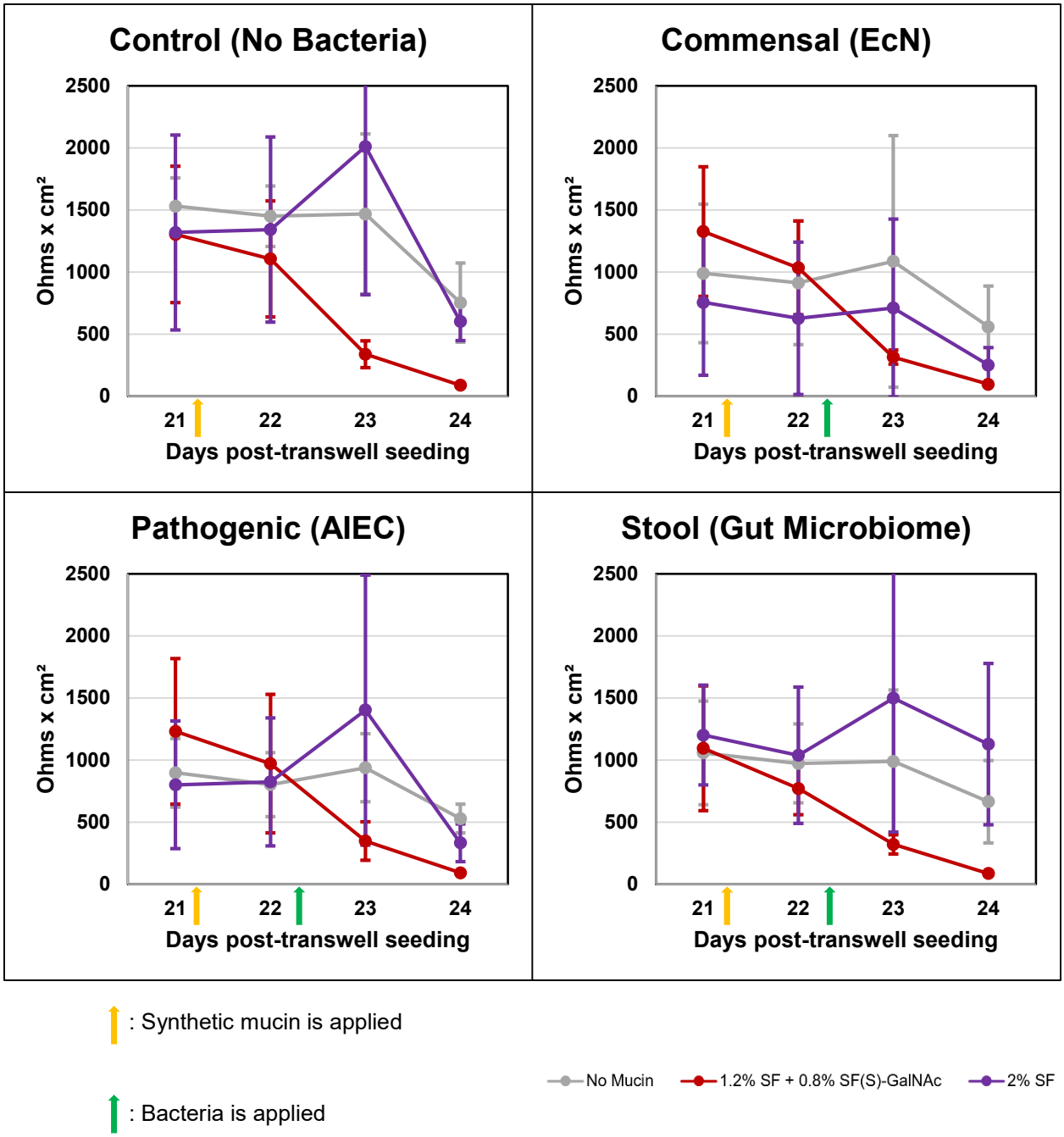

Figure 9: TEER Measurements taken of Caco-2 cells in transwells. Caco-2 transwells were separated into 4 bacteria groups: No bacteria, commensal bacteria (EcN), and pathogenic bacteria (AIEC), and stool (full gut microbiome). Caco-2 transwells were also divided into 3 separate mucin groups: No mucin, 1.2% SF + 0.8% SF(S)-GalNAc, and 2% SF. Synthetic mucin was applied 21 days post-transwell seeding. Bacteria was applied 22 days post-transwell seeding. In the "Control" set, TEER for all groups except

Control-2% SF decreased significantly from Day 21 to Day 24. In the “Commensal”, “Pathogenic”, and “Stool” sets, only “1.2% SF + 0.8% SF(S)-GalNAc” TEER decreased significantly from Day 21 to Day 24.

Following TEER measurements, all samples were immunostained for confocal imaging. Noticeable ZO-1 expression was observed among all samples. Weak ZO-1 expression was observed among “No mucin” samples, except for the “Stool” sample. Strong ZO-1 expression was observed for all “1.2% SF + 0.8% SF(S)-GalNAc” samples, which was demonstrated by the clear chicken-wire pattern of tight junctions between cells. These results for “1.2% SF + 0.8% SF(S)-GalNAc” were surprising, considering that TEER decreased over time for this mucin groups across all bacteria sets. Decent ZO-1 expression was observed among all “2% SF” samples exposed to bacteria, with especially strong expression in the Commensal-2% SF sample (Figure 10).

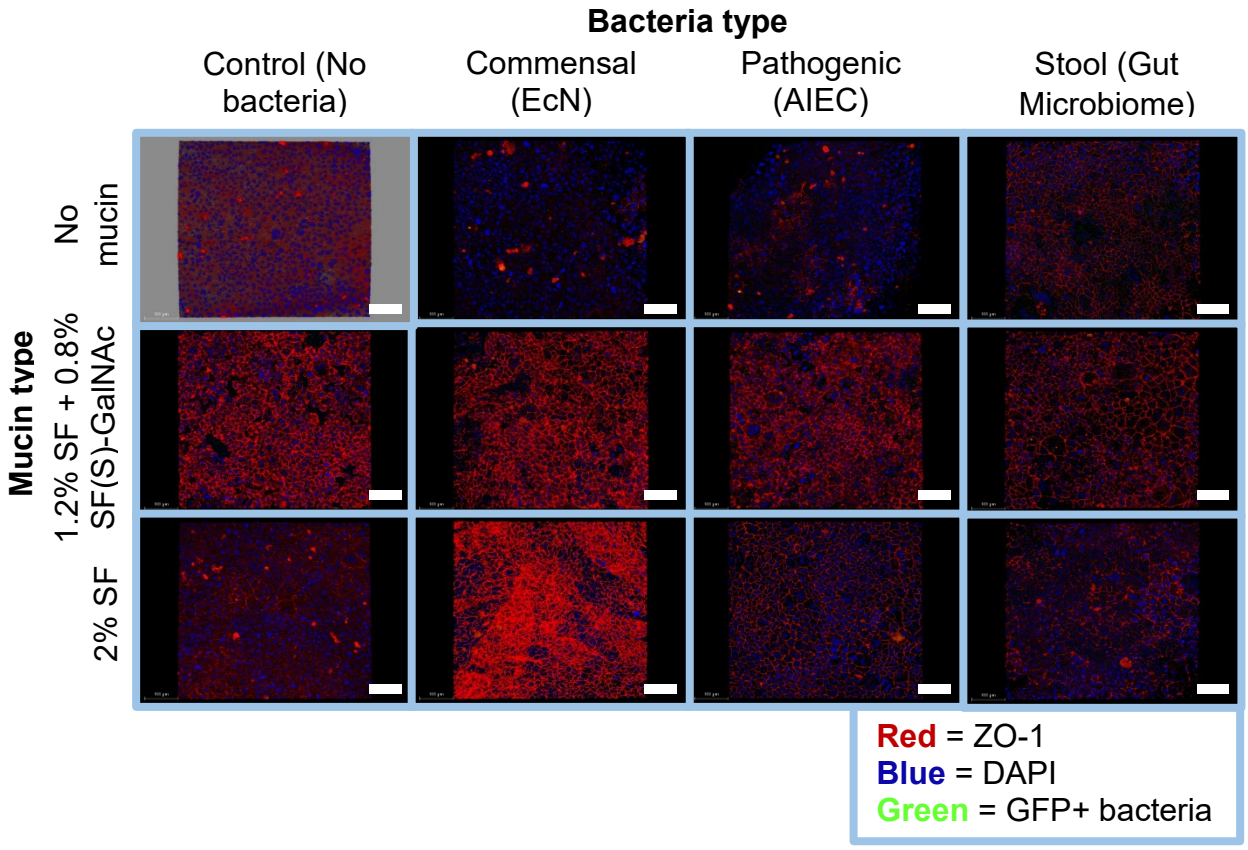

Figure 10: Confocal images taken of Caco-2 cells. Images were taken at 20x magnification. Caco-2 transwells were separated into 4 bacteria groups: No bacteria, commensal bacteria (EcN), and pathogenic bacteria (AIEC), and stool (full gut microbiome). Caco-2 transwells were also divided into 3 separate mucin groups: No mucin, 1.2% SF + 0.8% SF(S)-GalNAc, and 2% SF. In the "Control", "Commensal", and "Pathogenic" sets, strong Caco-2 monolayer integrity was observed in "1.2% SF + 0.8% SF(S)-GalNAc" and "2% SF" samples. Strong Caco-2 monolayer integrity was observed across all "Stool" samples. Scale bar = 100 μm

Results Summary (Experiment 3)

In the "Control" set, only "No mucin" and "1.2% SF + 0.8% SF(S)-GalNAc" TEER decreased significantly from Day 21 to Day 24. In the "Commensal", "Pathogenic", and "Stool" sets, only "1.2% SF + 0.8% SF(S)-GalNAc" TEER significantly decreased from Day 21 to Day 24. However, despite "No mucin" TEER being highest at Day 24 in the "Commensal" and "Pathogenic" sets, "No mucin" confocal samples in these sets exhibited noticeably weaker monolayer integrity than in "1.2% SF + 0.8% SF(S)-GalNAc" and "2% SF" samples. All confocal "Stool" samples exhibited strong monolayer integrity. For all bacteria groups, "1.2% SF + 0.8% SF(S)-GalNAc" TEER reached below 100 Ohms x cm^2 by Day 24. However, based on confocal imaging, "1.2% SF + 0.8% SF(S)-GalNAc" samples still exhibited strong monolayer integrity in all bacteria groups and was strongest amongst "Control" samples.

4d. Experiment 4: Testing Other Silk-Sugar Synthetic Mucins

In this experiment, two new silk-sugar synthetic mucins, "1.4% SF + 0.6% SF(D, E)-GalNAc" and "1.4% SF + 0.6% SF(S)-GalN", were tested as well as "2% SF" from previous experiments. 5 replicates were used for each mucin group within each bacteria

group. Synthetic mucin was applied immediately after Day 19 measurements and bacteria was applied immediately after Day 21 measurements. In the “Control” set, “2% SF” followed by “1.4% SF + 0.6% SF(D, E)-GalNAc” seemingly performed better than “1.4% SF + 0.6% SF(S)-GalN”, following mucin application. However, no significant differences were found between mucin groups at all days. Additionally, for each mucin group, no significant differences were found between days. In the “Commensal” set, no significant differences were found between mucin groups at all days. A significant increase in TEER was observed for “1.4% SF + 0.6% SF(D, E)-GalNAc” following synthetic mucin application, between Day 19 and Day 20. TEER also increased from Day 19 and 20 for the other mucin groups, although this increase was not considered significant. For all mucin groups, TEER decreased from Day 21 to Day 23, but this decrease was only significant for the “1.4% SF + 0.6% SF(S)-GalN” and “1.4% SF + 0.6% SF(D, E)-GalNAc” groups. In the “Pathogenic” set, no significant differences were observed between mucin groups at all days except Day 23. Regardless, Day 23 TEER for all mucin groups fell below the minimum TEER associated with strong Caco-2 monolayer integrity [34]. Before bacteria application, no significant differences were observed between days for each mucin group (Figure 11).

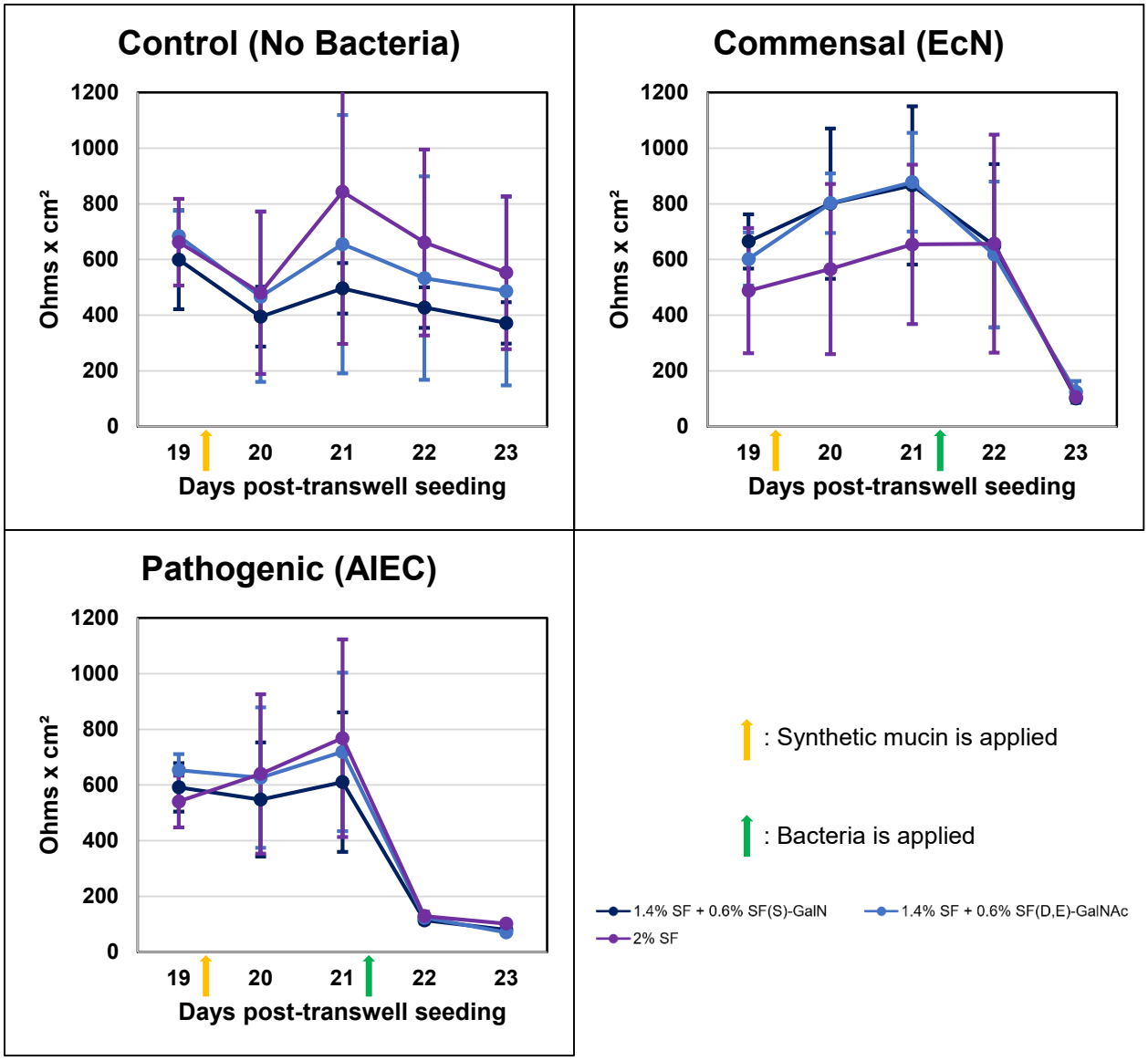

Figure 11: TEER Measurements taken of Caco-2 cells in transwells. Caco-2 transwells were separated into 3 bacteria groups: No bacteria, commensal bacteria (EcN), and pathogenic bacteria (AIEC). Caco-2 transwells were also divided into 3 separate synthetic mucin groups: 1.4% SF + 0.6% SF(S)-GalN, 1.4% SF + 0.6% SF(D, E)-GalNAc, and 2% SF. Synthetic mucin was applied 19 days post-transwell seeding. Bacteria was applied 21 days post-transwell seeding. TEER for all "Control" groups remained stable from Day 19 to Day 23. TEER for all "Commensal" and "Pathogenic" groups decreased significantly from Day 19 to Day 23.

In the “Control” samples, a faint chicken-wire pattern was observed in the “1.4% SF + 0.6% SF(D, E)-GalNAc” sample and a stronger pattern was observed in the “2% SF” sample. A faint chicken-wire pattern was also observed in “Commensal” samples, but with less DAPI expression compared to the “Control” samples. For the silk-sugar “Pathogenic” samples, despite some ZO-1 expression, the chicken-wire structure of tight junctions appeared compromised. The Pathogenic-2% SF sample’s composition was unclear, which could have been caused by auto fluorescence of the transwell membrane (Figure 12).

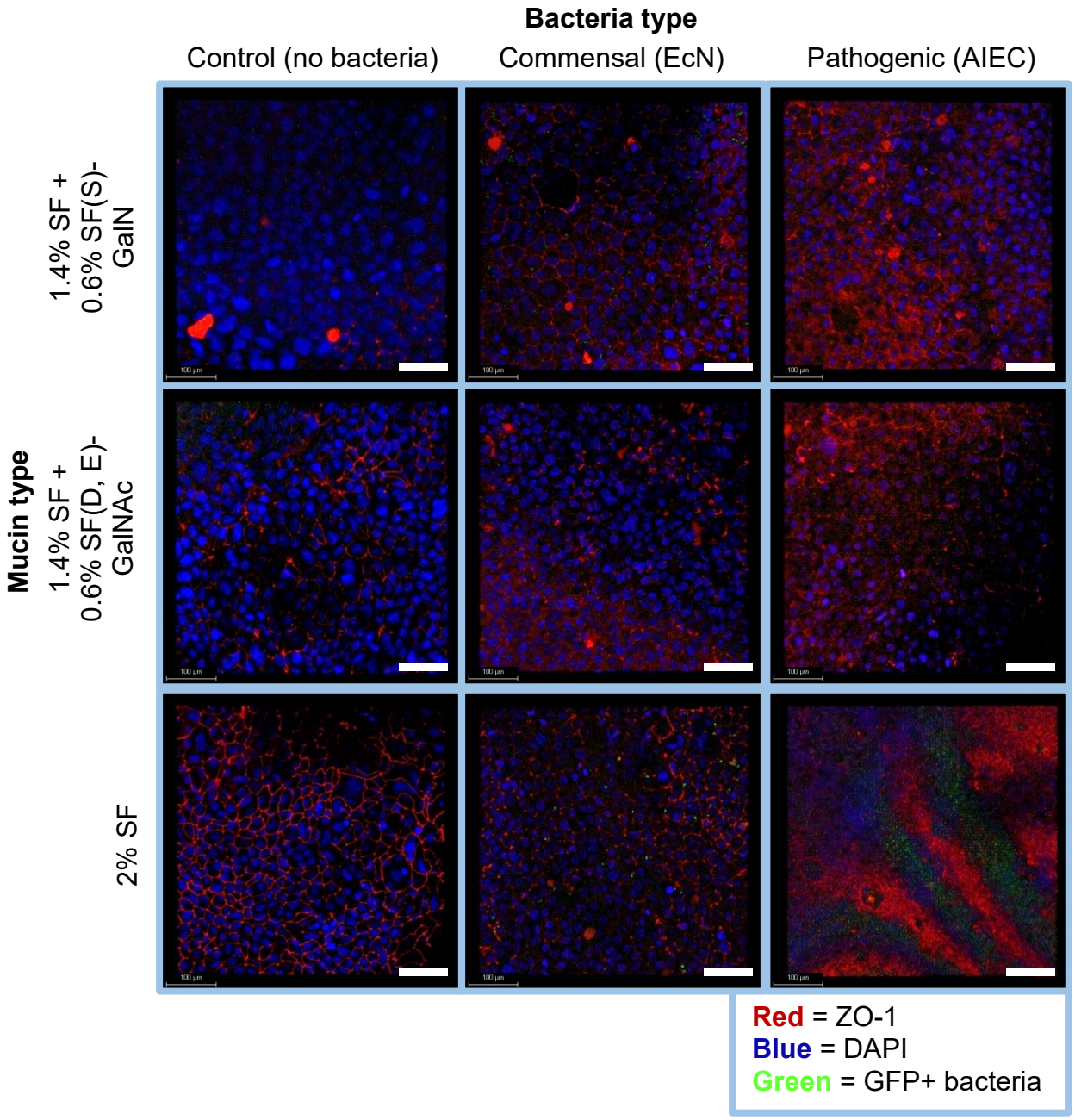

Figure 12: Confocal images taken of Caco-2 cells. Images were taken at 20x magnification. Caco-2 transwells were separated into 3 bacteria groups: No bacteria, commensal bacteria (EcN), and pathogenic bacteria (AIEC). Caco-2 transwells were also divided into 3 separate synthetic mucin groups: 1.4% SF + 0.6% SF(S)-GalN, 1.4% SF + 0.6% SF(D, E)-GalNAc, and 2% SF. In the "Control" set, decent Caco-2 monolayer integrity was only visible in Control-1.4% SF + SF(D, E)-GalNAc and -2% SF. In the "Commensal" set, decent monolayer integrity was only visible in Commensal-1.4% SF + 0.6% SF(S)-

GalN and -2% SF. All “Pathogenic samples exhibited at least some monolayer compromise. Scale bar = 100 µm

Unlike in the previous experiments, Caco-2 monolayers were visible in samples under SEM imaging. Normally, differentiated Caco-2 cells possess a dense apical brush border of micro-villi as well as tight junctions, all of which would be visible under SEM. Additionally, Caco-2 cells self-assemble into a hexagonal arrangement [40]. Cracks between cells could have been the result of SEM sample preparation [41]. In this experiment, monolayers were visible in the Control-1.4% SF + 0.6% SF(D, E)-GalNAc and Control-2% SF samples as well as all “Commensal” samples. In the Control-1.4% SF + 0.6% SF(S)-GalNAc sample, a monolayer may have been visible under what appeared to be residual synthetic mucin. Bacteria seemed to have overwhelmed the Caco-2 monolayers in the “Pathogenic” samples. Bacteria were identified as rod-shaped *E. coli* ~1 µm in length. Microvilli were visible atop cells in “Control” and “Commensal” samples, however, it was difficult to identify tight junctions and separation between individual cells. Where cracks in monolayers could been seen, tight junctions between cells may have existed before samples were prepared for SEM. In “Control” samples, microvilli did not appear densly packed as well (Figure 13).

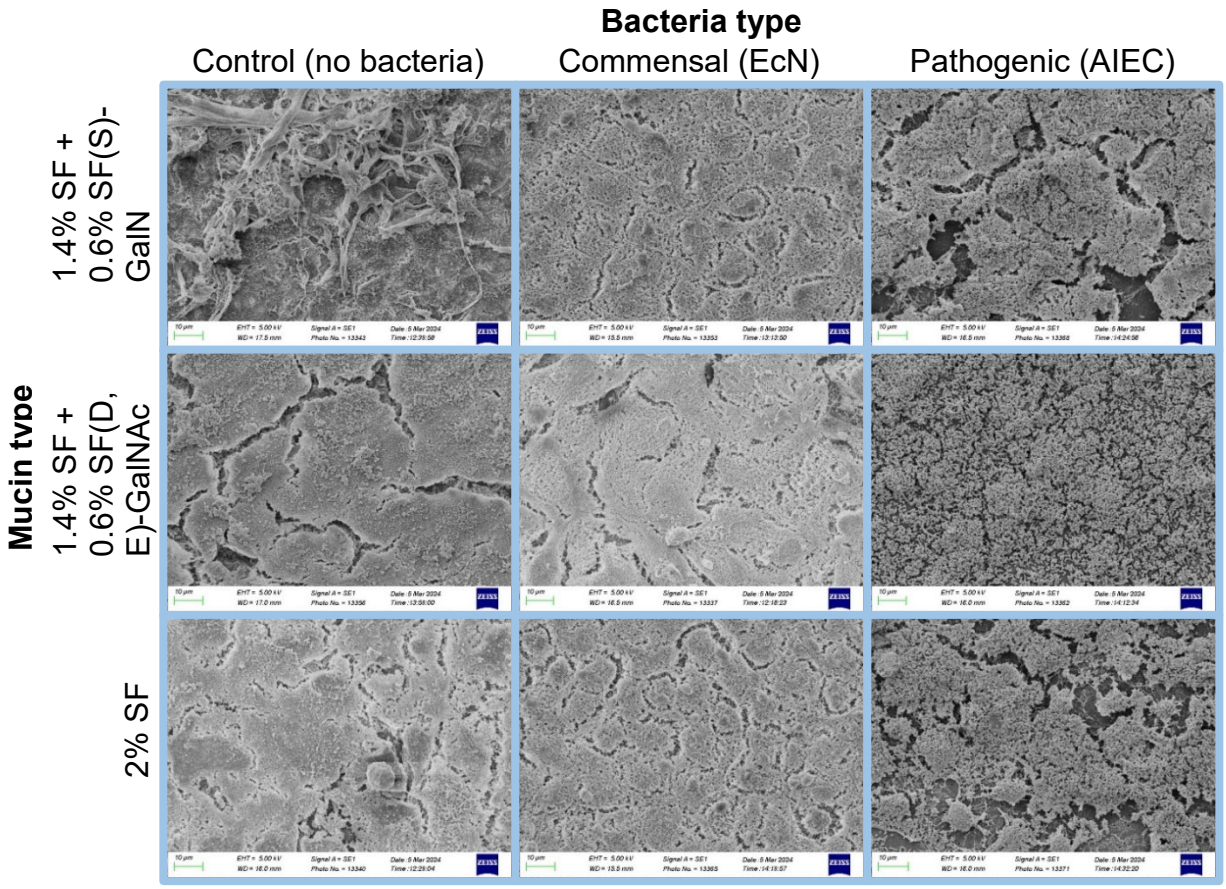

Figure 13: SEM images of Caco-2 cells. Caco-2 transwells were separated into 3 bacteria groups: No bacteria, commensal bacteria (EcN), and pathogenic bacteria (AIEC). Caco-2 transwells were also divided into 3 separate synthetic mucin groups: 1.4% SF + 0.6% SF(S)-GalN, 1.4% SF + 0.6% SF(D, E)-GalNAc, and 2% SF. Strong Caco-2 monolayers were visible in all "Control" and "Commensal" samples, except Control-No mucin where the mucin layer was mostly visible. Bacteria infiltration was observed across all "Pathogenic" samples. Scale bars at the bottom left of each image read "10 µm".

Results Summary (Experiment 4)

In the "Control" set, no significant differences in TEER for all mucin groups was observed from Day 19 to Day 23. TEER for all mucin groups remained above the minimum TEER associated with strong Caco-2 monolayer integrity (200 Ohms x cm^2) [34]. A chicken-wire pattern was visible for the Control-1.4% SF + 0.6% SF(D, E)-

GalNAc and Control-2% SF confocal samples and monolayers were visible for the equivalent SEM samples. In the “Commensal” set, TEER decreased significantly for all mucin groups following bacteria application, dropping below 200 Ohms x cm^2. Although, faint chicken-wire patterns were still observed in the Commensal-1.4% SF + 0.6% SF(S)-GalN and Commensal-2% SF confocal samples and monolayers were visible for the corresponding SEM samples as well. In the “Pathogenic” set, TEER for all mucin groups decreased significantly following bacteria application, dropping below 200 Ohms x cm^2. A chicken-wire pattern was not observed in “Pathogenic” confocal samples. Bacteria seemed to have overwhelmed monolayers in Pathogenic SEM samples as well.

4e. Experiment 5: Assessing Impact of Synthetic Mucins at Different Time Points using Confocal Imaging

Porcine mucin was introduced in this experiment as a positive control. In other words, porcine mucin was expected to perform well and maintain Caco-2 monolayer integrity even after bacteria application. The results of this experiment, however, indicated that porcine mucin could not maintain monolayer integrity. 4 replicates were used for each mucin group within each bacteria group. Synthetic mucin was applied immediately after Day 10 measurements and bacteria was applied immediately after Day 12 measurements. In the “Control” set, TEER for “No mucin” remained stable throughout the experiment; no significant difference was observed between days of any “No mucin” measurements. When comparing “No mucin” with the other mucin groups, no significant differences in TEER were observed at all days. For the “2% porcine mucin”, “1.4% SF + 0.6% SF(D, E)-GalNAc”, and “2% SF” mucin groups, a significant

decrease in TEER was observed between Day 10 and Day 14. Since TEER measurements between “No mucin” and other mucin groups at every day were not significantly different, the data suggested that the addition of these synthetic mucins did not improve Caco-2 monolayer integrity. In the “Commensal” set, there were no significant differences between “No mucin” and other mucin groups before bacteria application (Day 13). While significant differences were found between some mucin groups post-bacteria application, all TEER measurements fell below 200 Ohms x cm^2. All mucin groups experienced a significant decrease in TEER from Day 10 to Day 13. For all mucin groups, no significant differences in TEER over time were found before bacteria application. In the “Pathogenic” set, no significant differences were found between “No mucin” and other mucin groups at all days, except for between “No mucin” and “2% SF at Day 11. Like the “Commensal” set, all mucin groups in the” Pathogenic” set experienced a significant decrease in TEER from Day 10 to Day 13. From Day 12 to Day 13, significant decreases in TEER were observed only for “2% porcine mucin”, “1.4% SF + 0.6% SF(S)-GalN”, and “2% SF”. No significant differences in TEER were found for all mucin groups before bacteria application (Figure 14).

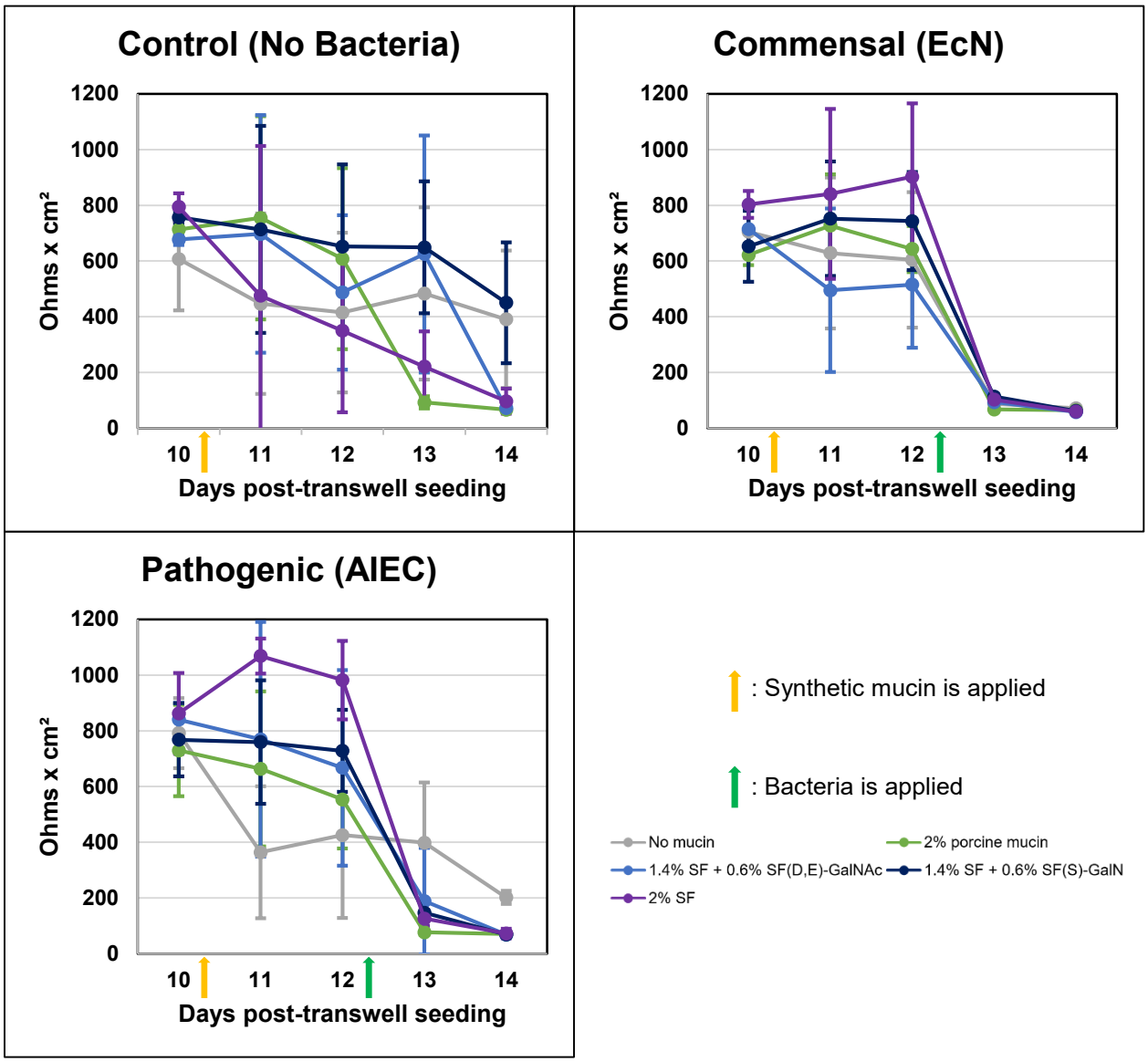

Figure 14: TEER Measurements taken of Caco-2 cells in transwells. Caco-2 transwells were separated into 3 bacteria groups: No bacteria, commensal bacteria (EcN), and pathogenic bacteria (AIEC). Caco-2 transwells were also divided into 5 separate mucin groups: No mucin, 2% porcine mucin, 1.4% SF + 0.6% SF(S)-GalN, 1.4% SF + 0.6% SF(D, E)-GalNAc, and 2% SF. Synthetic mucin was applied 10 days post-transwell seeding. Bacteria was applied 12 days post-transwell seeding. TEER for all "Control" groups decreased from Day 10 to Day 14, with only Control-2% porcine mucin TEER decreasing significantly.

TEER for all “Commensal” and “Pathogenic” groups, except Pathogenic-No mucin, decreased significantly from Day 10 to Day 14.

24-hour samples were immunostained after Day 13 TEER measurements. “Control” samples had stronger ZO-1 expression compared to “Commensal” or “Pathogenic” samples. The chicken-wire pattern of Caco-2 monolayers was visible in all “Control” samples and most marked in the non-porcine mucin samples. The strong ZO-1 expression and chicken-wire pattern in these samples was indicative of strong monolayer integrity. ZO-1 expression was weaker in “Commensal” samples and the chicken-wire pattern of Caco-2 monolayers was not identifiable. Additionally, only small clumps of cells were identifiable for “Commensal” samples. This indicated that Caco-2 monolayers detached from transwell membranes due to bacteria exposure and were compromised by the bacteria. Similar clumps of cells were identifiable for all “Pathogenic” samples, except “No mucin” and “2% porcine mucin” samples. Surprisingly, decent monolayer integrity and a chicken-wire pattern was identifiable in the Pathogenic-No mucin group (Figure 15).

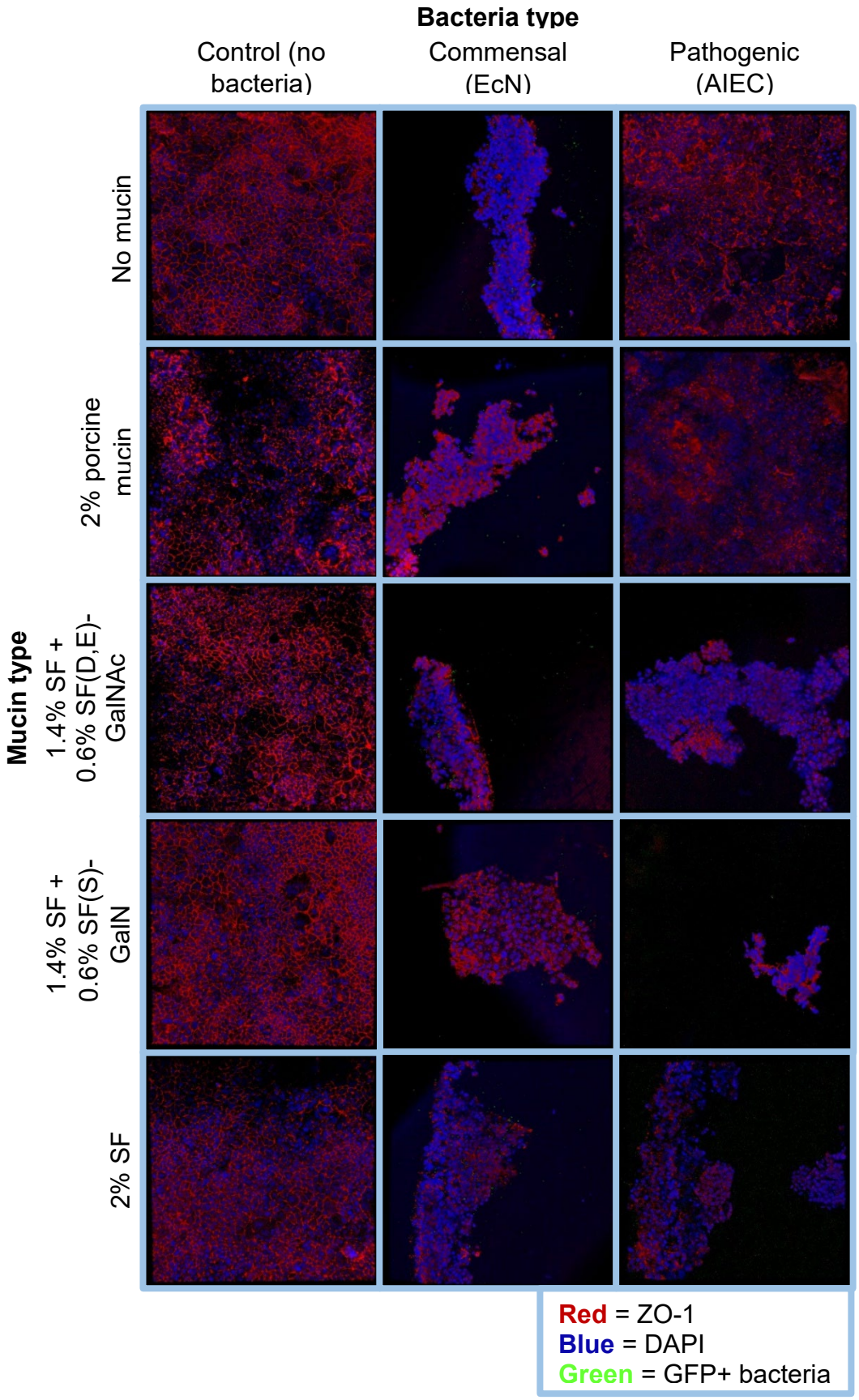
Bacteria type
Control (no bacteria)
Commensal (EcN)
Pathogenic (AIEC)
Mucin type
No mucin
2% porcine mucin
1.4% SF + 0.6% SF(D,E)-GalNAc
1.4% SF + 0.6% SF(S)-GalN
2% SF
Red = ZO-1
Blue = DAPI
Green = GFP+ bacteria

Figure 15: Confocal images taken of Caco-2 cells stained at **24 hours' post-bacteria application**. Images were taken at 20x magnification. Caco-2 transwells were separated into 3 bacteria groups: No bacteria, commensal bacteria (EcN), and pathogenic bacteria (AIEC). Caco-2 transwells were also divided into 5 separate mucin groups: No mucin, 2% porcine mucin, 1.4% SF + 0.6% SF(S)-GalN, 1.4% SF + 0.6% SF(D, E)-GalNAc, and 2% SF. All "Control" samples exhibited strong Caco-2 monolayer integrity, except Control-2% porcine mucin. All "Commensal" and "Pathogenic" samples exhibited monolayer degradation, except Pathogenic-No mucin. Scale bar = 100 μm

48-hour samples were immunostained after Day 14 TEER measurements. Overall, the samples stained 48 hours' post-bacteria application exhibited lower monolayer integrity than samples stained 24 hours' post-bacteria application. In the "Commensal" set, strong monolayer integrity was observed in the "No mucin", "1.4% SF + 0.6% SF(S)-GalN", and "2% SF" samples, evidenced by strong ZO-1 expression and an identifiable chicken-wire pattern. Strong monolayer integrity was not observed in any of the "Commensal" and "Pathogenic" samples, except for the Pathogenic-No mucin sample. In some samples such as the Commensal-2% porcine mucin and Pathogenic-2% porcine mucin samples, ZO-1 and DAPI expression was visible, however, the lack of a chicken-wire pattern of cells indicated that bacteria still compromised monolayers in these samples (Figure 16).

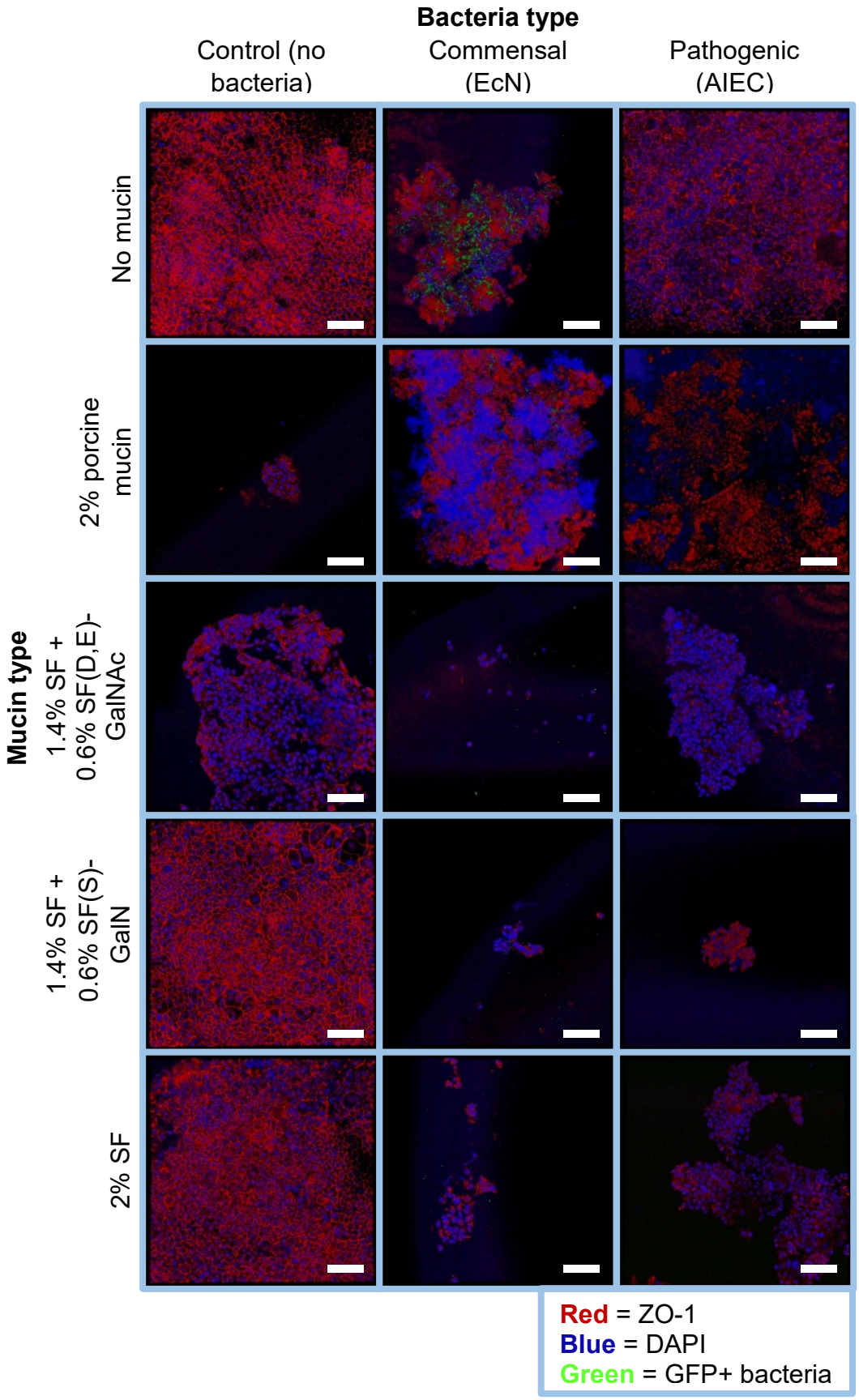
Bacteria type
Control (no bacteria)
Commensal (EcN)
Pathogenic (AIEC)
Mucin type
No mucin
2% porcine mucin
1.4% SF + 0.6% SF(D,E)-GalNAc
1.4% SF + 0.6% SF(S)-GalN
2% SF
Red = ZO-1
Blue = DAPI
Green = GFP+ bacteria

Figure 16: Confocal images taken of Caco-2 cells stained at **48 hours' post-bacteria application**. Images were taken at 20x magnification. Caco-2 transwells were separated into 3 bacteria groups: No bacteria, commensal bacteria (EcN), and pathogenic bacteria (AIEC). Caco-2 transwells were also divided into 5 separate mucin groups: No mucin, 2% porcine mucin, 1.4% SF + 0.6% SF(S)-GalN, 1.4% SF + 0.6% SF(D, E)-GalNAc, and 2% SF. In the "Control" set, decent Caco-2 monolayer integrity was visible only in Control-1.4% SF + 0.6% SF(S)-GalN and -2% SF. All "Commensal" and "Pathogenic" samples exhibited monolayer degradation, except Pathogenic-No mucin. Scale bar = 100 μm

Results Summary (Experiment 5)

In the "Control" set, TEER decreased for all mucin groups from Day 10 to Day 14 and this decrease was significant for "2% porcine mucin". However, all 24-hour "Control" mucin samples, except "2% porcine mucin", exhibited strong ZO-1 expression and chicken-wire pattern which were indicative of strong monolayer integrity. Among 48-hour "Control" confocal samples, monolayer integrity had worsened, but "1.4% SF + 0.6% SF(S)-GalN" and "2% SF" samples still exhibited a chicken-wire pattern. In the "Commensal" set, TEER for all mucin groups significantly decreased following bacteria application, dropping below 200 Ohms x cm^2. All 24- and 48-hour "Commensal" samples exhibited monolayer compromise possibly due to bacteria infiltration. In the "Pathogenic" set, with the exception of "No mucin", TEER for all mucin groups also decreased significantly following bacteria application, dropping below 200 Ohms x cm^2. 24- and 48-hour "Pathogenic" samples exhibited monolayer compromise as well. However, Pathogenic-No mucin TEER remained within healthy levels and exhibited decent monolayer integrity, even in the 48-hour confocal sample.

4f. Experiment 6: Comparing Impact of all Silk-Sugar Synthetic Mucins

In this experiment, “1.4% SF + 0.6% SF(S)-GalNAc” synthetic mucin was tested alongside the 5 mucins tested in the previous experiment. 4 replicates were used for each mucin group within each bacteria group. Synthetic mucin was applied immediately after Day 13 measurements and bacteria was applied immediately after Day 14 measurements. In the “Control” set, for all days except Day 15, no significant differences were found when comparing “No mucin” with other mucin groups. At Day 15, “2% porcine mucin” and “1.4% SF + 0.6% SF(S)-GalNAc" TEERs were significantly lower than “No mucin” TEER. “No mucin” TEER remained stable throughout the experiment; no significant differences in “No mucin” TEER were observed between days. From Day 15 to Day 16, TEER decreased for all mucin groups, however this decrease was not significant for any groups, possibly because sample size (number of replicates) decreased from 4 to 2. Overall, from Day 13 to Day 16, TEER for all mucin groups decreased at least slightly. In the “Commensal” set, no significant differences were found in TEER when comparing “No mucin” with other mucin groups on Day 13 and Day 14. On Day 15 and Day 16, “No mucin” TEER was greater than TEER for all other mucin groups, however, this difference was only significant when comparing “No mucin” with “2% porcine mucin” and “1.4% SF + 0.6% SF(S)-GalNAc” respectively on Day 15. From Day 14 to Day 15, a significant decrease in TEER was observed for all mucin groups except for “No mucin”. In the “Pathogenic” set, there were no significant differences in TEER between “No mucin” and other mucin groups at all days. For all mucin groups except “No mucin”, there was a significant decrease in TEER from Day 14 to Day 15 (Figure 17).

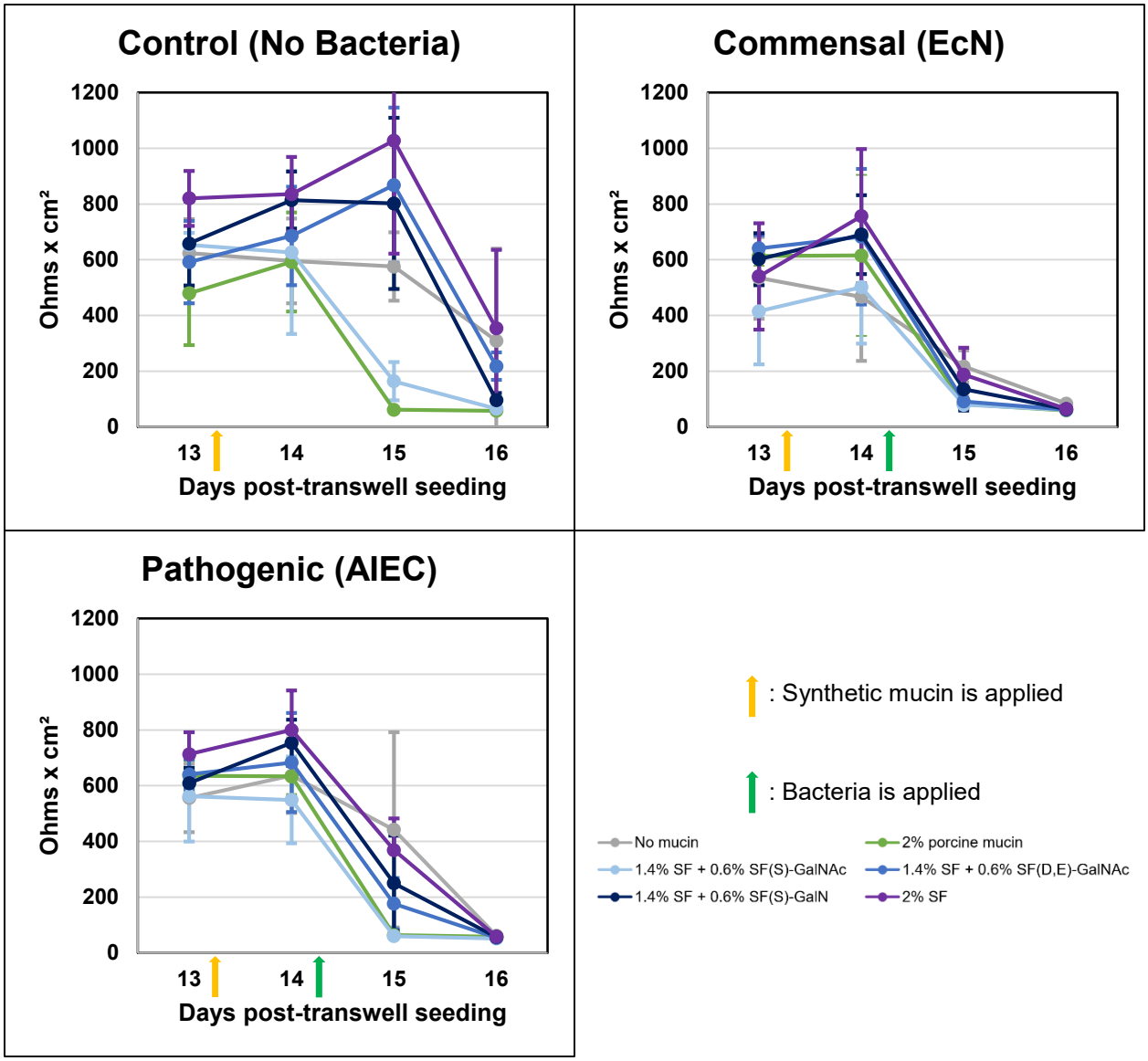

Figure 17: TEER Measurements taken of Caco-2 cells in transwells. Caco-2 transwells were separated into 3 bacteria groups: No bacteria, commensal bacteria (EcN), and pathogenic bacteria (AIEC). Caco-2 transwells were also divided into 6 separate mucin groups: No mucin, 2% porcine mucin, 1.4% SF + 0.6% SF(S)-GalNAc, 1.4% SF + 0.6% SF(D, E)-GalNAc, 1.4% SF + 0.6% SF(S)-GalN, and 2% SF. Synthetic mucin was applied 13 days post-transwell seeding. Bacteria was applied 14 days post-transwell seeding. TEER for all "Control" groups decreased from Day 13 to Day 16, with only Control-2% porcine mucin and Control-1.4% SF + 0.6% SF(S)-GalNAc decreasing significantly. TEER for all "Commensal" and

"Pathogenic" groups decreased significantly from Day 13 to Day 16, except Commensal- and Pathogenic-No mucin where TEER decrease was not significant.

24-hour samples were immunostained after Day 15 TEER measurements. In the "Control" samples, strong ZO-1 expression and an identifiable "chicken-wire" Caco-2 monolayer arrangement were observed across all samples except for "2% porcine mucin". A chicken-wire pattern of cells with decent ZO-1 expression was also observed for all "No mucin" and "2% SF" samples, across all bacteria groups, as well as the Pathogenic-1.4% SF + 0.6% SF(D, E)-GalNAc sample. These characteristics were especially surprising in the Pathogenic-No mucin group since no mucin was applied to protect cells from bacteria. The remaining samples exhibited signs of the Caco-2 monolayers compromise in the presence of bacteria, or in the presence of porcine mucin in the case of the "2% porcine mucin" samples. In these samples, the majority of Caco-2 cells were destroyed and dislodged from the transwell membranes because of exposure to incompatible substances. In these samples, the synthetic mucins were not sufficient in protecting Caco-2 cells from bacteria and maintaining monolayer integrity (Figure 18).

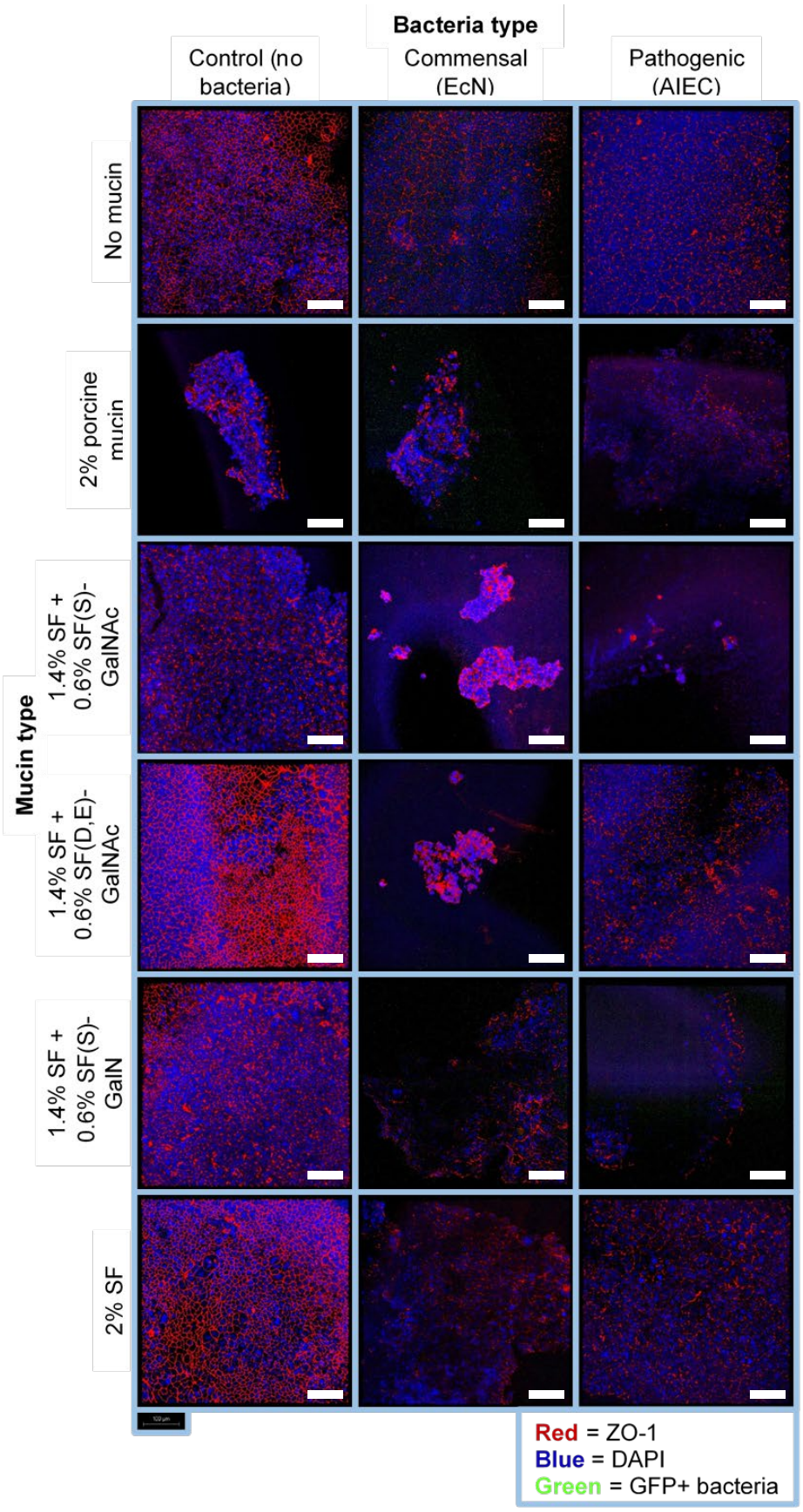
Bacteria type
Control (no bacteria)
Commensal (EcN)
Pathogenic (AIEC)
Mucin type
No mucin
2% porcine mucin
1.4% SF + 0.6% SF(S)-GalNAc
1.4% SF + 0.6% SF(D,E)-GalNAc
1.4% SF + 0.6% SF(S)-GalN
2% SF
Red = ZO-1
Blue = DAPI
Green = GFP+ bacteria

Figure 18: Confocal images taken of Caco-2 cells stained at **24 hours' post-bacteria application**. Images were taken at 20x magnification. Caco-2 transwells were separated into 3 bacteria groups: No bacteria, commensal bacteria (EcN), and pathogenic bacteria (AIEC). Caco-2 transwells were also divided into 6 separate mucin groups: No mucin, 2% porcine mucin, 1.4% SF + 0.6% SF(S)-GalNAc, 1.4% SF + 0.6% SF(D, E)-GalNAc, 1.4% SF + 0.6% SF(S)-GalN, and 2% SF. All "Control" samples exhibited strong Caco-2 monolayer integrity, except Control-2% porcine mucin. In the "Commensal" set, only Commensal-No mucin, -1.4% SF + SF(S)-GalN, and -2% SF exhibited at least decent monolayer integrity. In the "Pathogenic" set, only Pathogenic-No mucin, -1.4% SF + SF(D, E)-GalNAc, and -2% SF exhibited at least decent monolayer integrity. Scale bar = 100 μm

48-hour samples were immunostained after Day 16 TEER measurements. Compared to the cells of 24-hour samples, the cells of 48-hour samples were less viable. Similar to the 24-hour samples, the "Control" samples exhibited relatively strong ZO-1 expression and an identifiable "chicken-wire" Caco-2 monolayer arrangement, except for the "2% porcine mucin" and "1.4% SF + 0.6% SF(S)-GalNAc" samples. Decent ZO-1 expression was also observed Pathogenic-1.4% SF + 0.6% SF(D, E)-GalNAc sample however the chicken-wire pattern is not as noticeable. For the remaining samples, less viable and smaller clumps of cells were detected compared to their corresponding 24-hour samples. The 48-hour data overall suggested that even with synthetic mucin supplementation, cell viability decreased over time in the presence of bacteria (Figure 19).

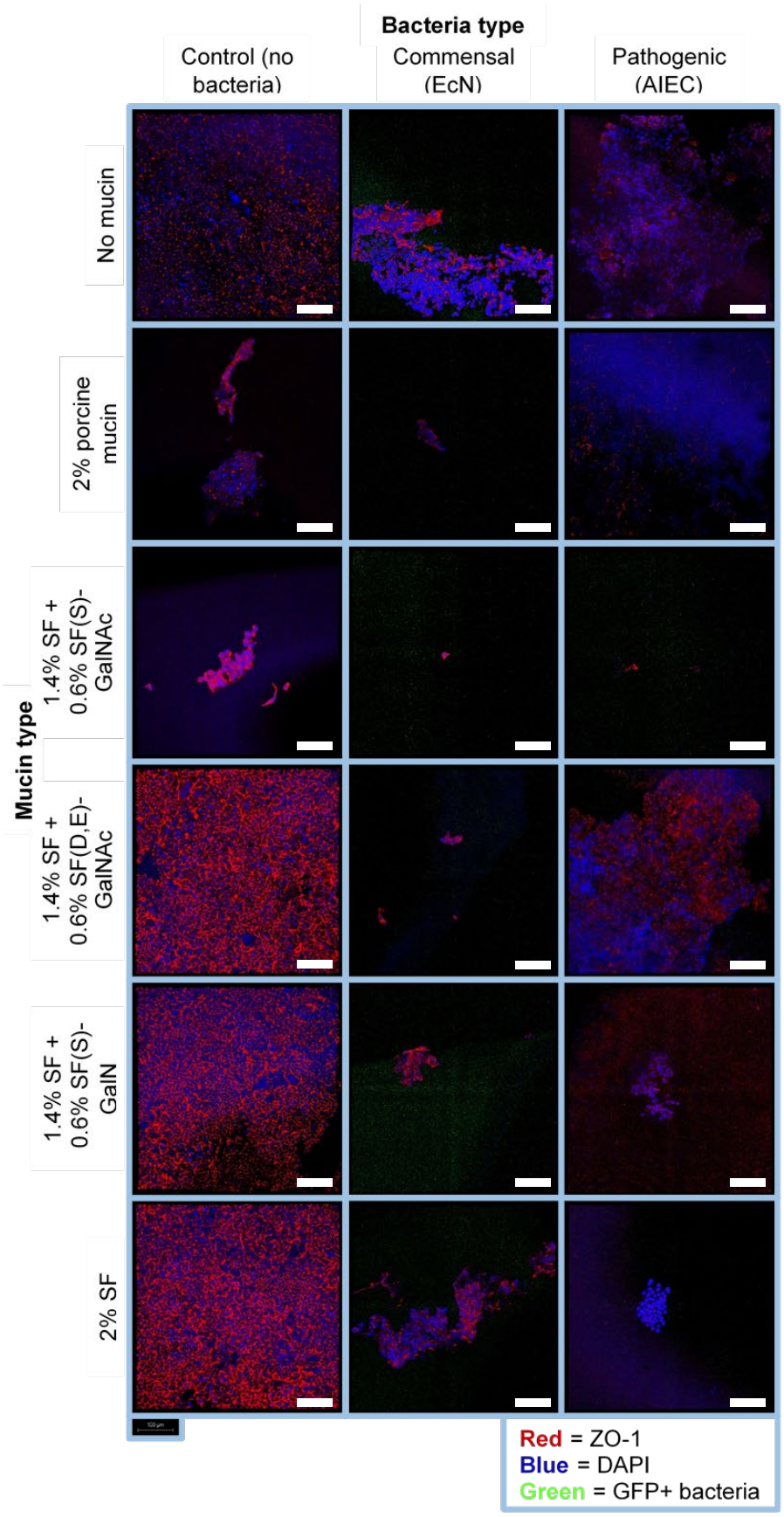
Bacteria type
Control (no bacteria)
Commensal (EcN)
Pathogenic (AIEC)
Mucin type
No mucin
2% porcine mucin
1.4% SF + 0.6% SF(S)-GalNAc
1.4% SF + 0.6% SF(D,E)-GalNAc
1.4% SF + 0.6% SF(S)-GalN
2% SF
Red = ZO-1
Blue = DAPI
Green = GFP+ bacteria

Figure 19: Confocal images taken of Caco-2 cells stained at **48 hours' post-bacteria application**. Images were taken at 20x magnification. Caco-2 transwells were separated into 3 bacteria groups: No bacteria, commensal bacteria (EcN), and pathogenic bacteria (AIEC). Caco-2 transwells were also divided into 6 separate mucin groups: No mucin, 2% porcine mucin, 1.4% SF + 0.6% SF(S)-GalNAc, 1.4% SF + 0.6% SF(D, E)-GalNAc, 1.4% SF + 0.6% SF(S)-GalN, and 2% SF. All "Control" samples exhibited strong Caco-2 monolayer integrity, except Control-2% porcine mucin and -1.4% SF + 0.6% SF(S)-GalNAc. All "Commensal" and "Pathogenic" samples exhibited compromised monolayer integrity. Scale bar = 100 μm

Results Summary (Experiment 6)

In the "Control" set, TEER for all mucin groups decreased from Day 13 to Day 16, but this decrease was only significant for "2% porcine mucin" and "1.4% SF + 0.6% SF(S)-GalNAc" groups. All "Control" 24-hour confocal samples exhibited strong monolayer integrity, except the "2% porcine mucin" sample. 48-hour samples also exhibited strong monolayer integrity, except the "2% porcine mucin" and "1.4% SF + 0.6% SF(S)-GalNAc" samples. In the "Commensal" set, TEER for all mucin groups decreased significantly following bacteria application, but this decrease was not significant for "No mucin". Among 24-hour "Commensal" confocal samples, only "No mucin", "1.4% SF + SF(S)-GalN", and "2% SF" samples exhibited decent monolayer integrity and these mucin groups had the highest average TEERs at Day 15, albeit not significantly greater than TEER of other mucin groups. All 48-hour "Commensal" samples exhibited compromised monolayer integrity. In the "Pathogenic" set, TEER for all mucin groups decreased significantly following bacteria application, but this decrease was not significant for "No mucin". Among 24-hour "Pathogenic" confocal samples, only "No mucin", "1.4% SF + SF(D, E)-GalNAc", and "2% SF" samples exhibited decent

monolayer integrity. All 48-hour “Pathogenic” samples exhibited compromised monolayer integrity. Interestingly, “No mucin” average TEER was highest among all mucin groups after bacteria application and 24-hour “No mucin” samples exhibited strong monolayer integrity, for both the “Commensal” and “Pathogenic” sets.

4g. Experiment 7: Testing Increased Concentration of Synthetic Mucin

For this experiment, the mucins tested were of the same composition as those in the previous experiment. However, the total concentration of mucins was increased from 2% to 5% in this run. Native human mucins have a concentration range of 0.5% to 5%, so testing 5% synthetic mucin was considered biologically relevant, at least based on concentration [42]. 4 replicates were used for each mucin group within each bacteria group. Synthetic mucin was applied immediately after Day 17 measurements and bacteria was applied immediately after Day 18 measurements. In the “Control” set, “No mucin” TEER was stable across all days. When comparing “No mucin” with other mucin groups on Day 17 and Day 20, no significant differences in TEER were observed. However, at Day 20, average “No mucin” TEER is greater than TEER of all other mucin groups. The difference in TEER between “No mucin” and other mucin groups at Day 20 was not significant most likely because sample size was reduced by half for all mucin groups in order to image cells at different time points. TEERs for “3.5% SF + 1.5% SF(D, E)-GalNAc” and “3.5% SF + 1.5% SF(S)-GalN” were significantly greater than “No mucin” only at Day 18. TEER for “5% SF” was significantly greater than “No mucin” only at Day 19. From Day 17 to Day 18, TEER for all mucin groups increased, however, TEER for all mucin groups decreased to below “No mucin” TEER by Day 20. In the “Commensal” set, TEER for all mucin groups from Day 17 to Day 18 increased and this

increase was significant for “3.5% SF + 1.5% SF(S)-GalN” and “5% SF”. When compared to “No mucin” TEER, “3.5% SF + 1.5% SF(S)-GalN” and “5% SF” TEERs were significantly higher on Day 18 while “3.5% SF + 1.5% SF(S)-GalNAc” TEER was significantly higher on Day 19. On Day 19, following bacteria application, TEER for all mucin groups decreased, however, TEERs for “3.5% SF + 1.5% SF(S)-GalNAc”, “3.5% SF + 1.5% SF(S)-GalN”, and “5% SF” were still significantly greater than TEER for “No mucin”. From Day 18 to Day 19, TEER decreased significantly for all mucin groups. In the “Pathogenic” set, TEER for each mucin group trended differently from Day 17 to Day 20. However, significant differences in TEER were only found on Day 18, when comparing “No mucin” to other mucin groups. At Day 18, “3.5% SF + 1.5% SF(S)-GalNAc”, “3.5% SF + 1.5% SF(D, E)-GalNAc”, and “5% SF” TEERs were significantly greater than “No mucin” TEER. Interestingly, TEER for “No mucin”, “3.5% SF + 1.5% SF(D, E)-GalNAc”, and “5% SF” either stayed level or increased from Day 18 to Day 19. In the same period, TEER for “5% porcine mucin”, “3.5% SF + 1.5% SF(D, E)-GalNAc”, and “3.5% SF + 1.5% SF(D, E)-GalN” decreased significantly. With the exception of TEER for Control-No mucin, TEER for all “Commensal” and “Pathogenic” mucin groups dropped below 200 Ohms x cm^2, which was considered the minimum TEER associated with strong monolayer integrity [34] (Figure 20).

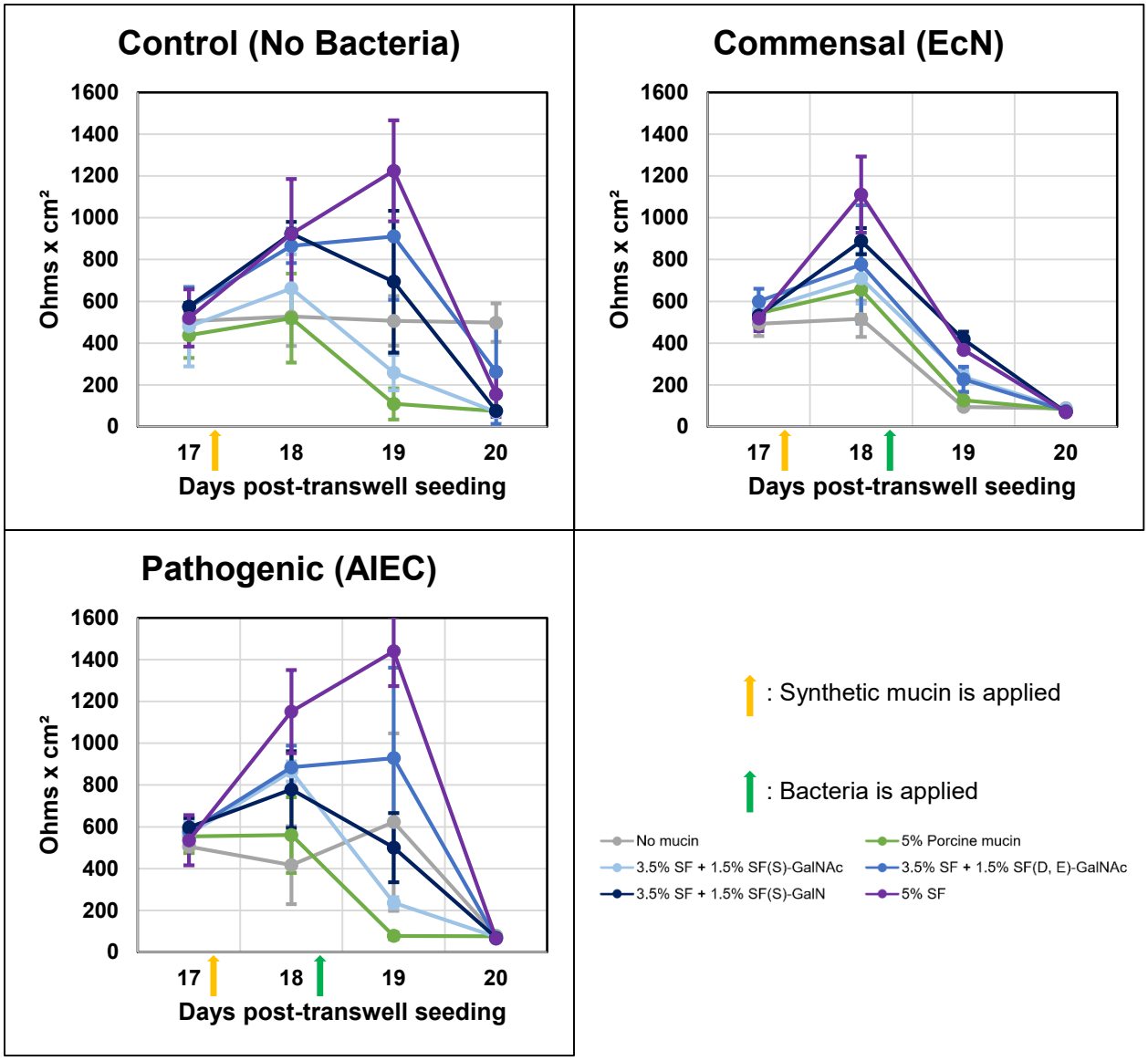

Figure 20: TEER Measurements taken of Caco-2 cells in transwells. Caco-2 transwells were separated into 3 bacteria groups: No bacteria, commensal bacteria (EcN), and pathogenic bacteria (AIEC). Caco-2 transwells were also divided into 6 separate mucin groups: No mucin, 5% porcine mucin, 3.5% SF + 1.5% SF(S)-GalNAc, 3.5% SF + 1.5% SF(D, E)-GalNAc, 3.5% SF + 1.5% SF(S)-GalN, and 5% SF. Synthetic mucin was applied 17 days post-transwell seeding. Bacteria was applied 18 days post-transwell seeding. TEER for all "Control" groups except Control-No mucin decreased from Day 17 to Day 20, with only Control-3.5% SF + 1.5% SF(S)-GalNAc decreasing significantly. TEER for all "Commensal" groups

decreased significantly from Day 17 to Day 20. TEER for all “Pathogenic” groups decreased from Day 17 to Day 20, with only Control-No mucin TEER decreasing significantly.

24-hour samples were immunostained after Day 19 TEER measurements. In the “Control” set, all samples exhibited strong ZO-1 expression and an identifiable “chicken-wire” arrangement of the Caco-2 monolayer. ZO-1 expression was especially strong in the “3.5% SF + 1.5% SF(D, E)-GalNAc” and “3.5% SF + 1.5% SF(S)-GalN” samples. In the “Commensal” set, all but the “No mucin” sample exhibited strong ZO-1 expression. In the case of the “3.5% SF + 1.5% SF(S)-GalNAc” sample, ZO-1 expression and a chicken-wire pattern were identified, however, DAPI-stained cells were not found. In the “Pathogenic” set, strong ZO-1 expression and a chicken-wire pattern were identified in the “3.5% SF + 1.5% SF(D,E)-GalNAc” sample, the “5% SF” sample, and notably the “No mucin” sample. Although, these characteristics were also identified in the Pathogenic-No mucin sample of the previous experiment. The “3.5% SF + 1.5% SF(S)-GalN” sample exhibited strong DAPI expression similar to healthy samples, but weak ZO-1 expression. This possibly demonstrated that Caco-2 cells could retain high viability despite monolayer integrity being compromised (Figure 21).

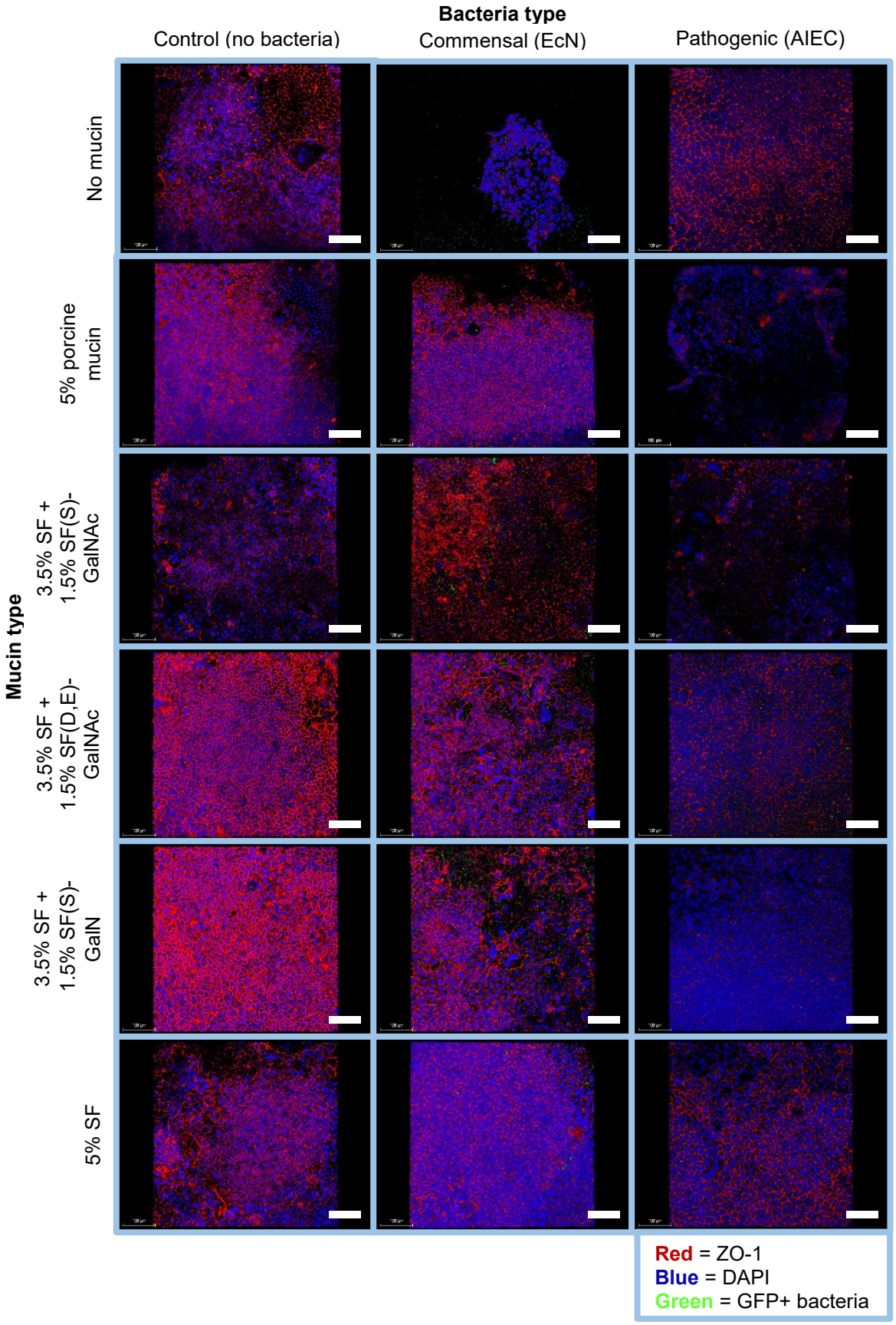
Bacteria type
Control (no bacteria)
Commensal (EcN)
Pathogenic (AIEC)
Mucin type
No mucin
5% porcine mucin
3.5% SF + 1.5% SF(S)-GalNAc
3.5% SF + 1.5% SF(D,E)-GalNAc
3.5% SF + 1.5% SF(S)-GalN
5% SF
Red = ZO-1
Blue = DAPI
Green = GFP+ bacteria

Figure 21: Confocal images taken of Caco-2 cells stained at **24 hours' post-bacteria application**. Images were taken at 20x magnification. Caco-2 transwells were separated into 3 bacteria groups: No bacteria, commensal bacteria (EcN), and pathogenic bacteria (AIEC). Caco-2 transwells were also divided into 6 separate mucin groups: No mucin, 5% porcine mucin, 3.5% SF + 1.5% SF(S)-GalNAc, 3.5% SF + 1.5% SF(D, E)-GalNAc, 3.5% SF + 1.5% SF(S)-GalN, and 5% SF. All "Control" samples exhibited strong Caco-2 monolayer integrity, except Control-5% porcine mucin" and -3.5% SF + 1.5% SF(S)-GalNAc which had decent monolayer integrity. All "Commensal" samples exhibited at least decent monolayer integrity, except Commensal-No mucin and -3.5% SF + 1.5% SF(S)-GalNAc. All "Pathogenic" samples exhibited at least decent monolayer integrity, except -5% porcine mucin and -3.5% SF + 1.5% SF(S)-GalNAc. Scale bar = 100 μm

48-hour samples were immunostained after Day 20 TEER measurements. For the 48-hour samples, the Control-No mucin, Control-3.5% SF + 1.5% SF(D,E)-GalNAc, and Control-5% SF samples all exhibited strong ZO-1 expression and chicken-wire patterns. Overall, however, 48-hour samples exhibited weaker ZO-1 expression and noticeable Caco-2 monolayer destruction compared to 24-hour samples. No "Commensal" or "Pathogenic" samples exhibited characteristics of a healthy monolayer. "Commensal" samples did possess larger clumps of cells than "Pathogenic" samples. However, the sparsity of the clumps still indicated that monolayer integrity was compromised in these samples. Essentially, these results further demonstrated that the ability of synthetic mucins to maintain Caco-2 monolayer integrity, even without bacteria presence, worsened over time (Figure 22).

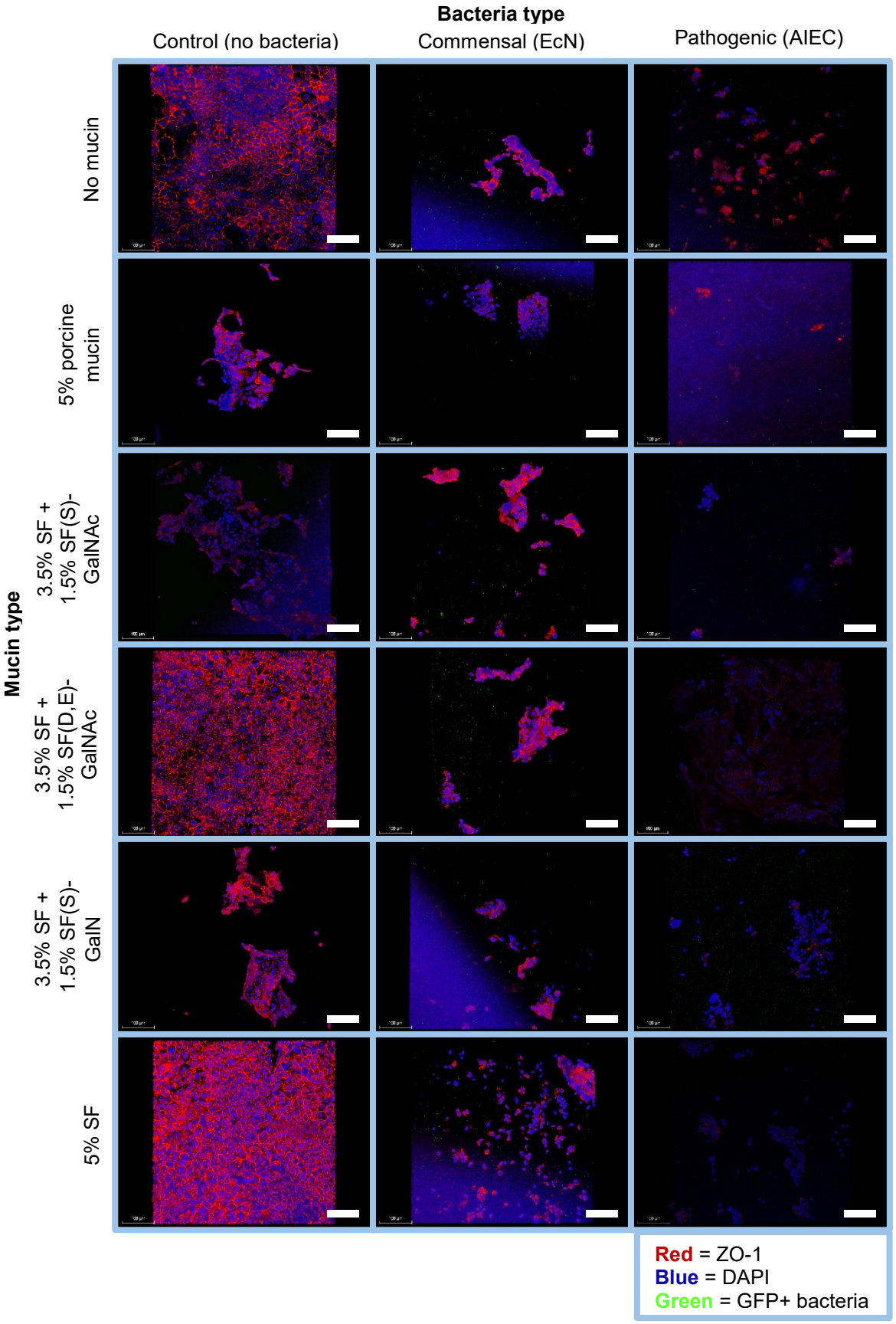
Bacteria type
Control (no bacteria)
Commensal (EcN)
Pathogenic (AIEC)
Mucin type
No mucin
5% porcine mucin
3.5% SF + 1.5% SF(S)-GalNAc
3.5% SF + 1.5% SF(D,E)-GalNAc
3.5% SF + 1.5% SF(S)-GalN
5% SF
Red = ZO-1
Blue = DAPI
Green = GFP+ bacteria

Figure 22: Confocal images taken of Caco-2 cells stained at **48 hours' post-bacteria application**. Images were taken at 20x magnification. Caco-2 transwells were separated into 3 bacteria groups: No bacteria, commensal bacteria (EcN), and pathogenic bacteria (AIEC). Caco-2 transwells were also divided into 6 separate mucin groups: No mucin, 5% porcine mucin, 3.5% SF + 1.5% SF(S)-GalNAc, 3.5% SF + 1.5% SF(D, E)-GalNAc, 3.5% SF + 1.5% SF(S)-GalN, and 5% SF. In the "Control" set, only Control-No mucin, -3.5% SF + 1.5% SF(D, E)-GalNAc, and -5% SF exhibited strong Caco-2 monolayer integrity. All "Commensal" and "Pathogenic" samples exhibited compromised monolayer integrity. Scale bar = 100 μm

Results Summary (Experiment 7)

In the "Control" set, TEERs for "5% porcine mucin" and "3.5% SF + 1.5% SF(S)-GalNAc" were significantly lower than other mucin groups at Day 19, which indicated that samples of these mucin groups had at least somewhat compromised monolayer integrity. This evidence was supported by 24-hour "Control" confocal data where chicken-wire patterns were less defined for "5% porcine mucin" and "3.5% SF + 1.5% SF(S)-GalNAc" samples compared to other "Control" samples. Notably, however, all "Control" samples still exhibited strong ZO-1 expression and decently defined chicken-wire patterns. In the "Commensal" set, TEER for all mucin groups significantly decreased following bacteria application. Among 24-hour "Commensal" samples,"5% porcine mucin, "3.5% SF + 1.5% SF(D, E)-GalNAc, "3.5% SF + 1.5% SF(S)-GalN", and "5% SF" samples exhibited at least decent monolayer integrity. In the "Pathogenic" set, TEERs for "No mucin", "3.5% SF + 1.5% SF(D, E)-GalNAc", 3.5% SF + 1.5% SF(S)-GalN", and "5% SF" remained above 200 Ohms x cm^2 following bacteria application, indicating strong monolayer integrity. This evidence was supported by strong ZO-1 expression and decent chicken-wire patterns found in corresponding 24-hour

“Pathogenic” confocal samples. For all 48-hour “Commensal” and “Pathogenic” samples, monolayer integrity was severely compromised. This was supported by “Commensal” and “Pathogenic” TEER data at Day 20, where TEER for all mucin groups was below 200 Ohms x cm^2.

5. Discussion

In this study, varying compositions and concentrations of synthetic mucin were screened. These synthetic mucins were screened for their ability to protect intestinal epithelial cells from bacteria and for their ability to support the healthy co-existence of cells and commensal bacteria. This study was meant to identify a synthetic mucin candidate that could satisfy these objectives. By implementing synthetic mucin into an *in vitro* intestinal epithelial model, this study was also meant to address the shortcomings of existing models that do not incorporate synthetic mucin or models that have used non-biologically relevant mucin. The current 2D transwell model, while not matching the relevance of other *in vitro* models in terms of 3D structure, aimed to improve on existing models by incorporating a mucin that could mimic the interactions between mucus, epithelial cells, and bacteria in the native human small intestine. Incorporating synthetic mucins creates opportunity for the study and co-culture of intestinal epithelial cells and bacteria. The study was able to confirm that synthetic mucins of silk-sugar composition were biocompatible with Caco-2 cells. The study also confirmed that the ability of these synthetic mucins to protect Caco-2 cells from bacteria diminishes over time. Whether the screened synthetic mucins could provide an effective barrier to protect cells from bacteria infiltration remains unclear. Some results suggested that certain synthetic mucins could maintain Caco-2 monolayer integrity in the presence of bacteria. However, other results suggested that these same synthetic mucins could not fulfill this objective.

5a. Synthetic Mucin Biocompatibility

Based on confocal imaging from experiments, all synthetic mucins tested were biocompatible with Caco-2 cells and could support monolayer formation.

Biocompatibility was assessed using the samples containing no bacteria. In these "Control" groups, Caco-2 and synthetic mucin interactions were observable longer than in samples containing bacteria, since bacteria would be applied only 1-2 days after synthetic mucin application. In Experiment 1, No bacteria-0.5% SF(S)-GalNAc and No bacteria-2% SF confocal samples exhibited strong DAPI and ZO-1 expression, which would indicate that Caco-2 cells could thrive in the presence of these synthetic mucins (Figure 1). In Experiment 3, Control-1.2% SF + 0.8% SF(S)-GalNAc samples also exhibited these characteristics (Figure 8). Control-1.4% SF + 0.6% SF(S)-GalNAc, Control-1.4% SF + 0.6% SF(D, E)-GalNAc, and Control -1.4% SF + 0.6% SF(S)-GalNAc samples all exhibited these characteristics as well in Experiment 6 (Figure 16). These results on biocompatibility confirm that synthetic mucins of silk/sugar do not prevent Caco-2 monolayers from developing strong monolayers and can be tuned in future studies.

5b. Assessing Impact of Synthetic Mucins at Different Time Points

In Experiments 5-7, samples were imaged using confocal microscopy at 2 different time points post-bacteria application: 24 hours' and 48 hours' post-bacteria application. This was done to visualize the effect of bacteria on Caco-2 monolayer integrity over time. In these last 3 experiments. confocal imaging revealed that Caco-2 monolayer integrity for "Commensal" and "Pathogenic" samples worsened from 24 to 48 hours, even in samples where synthetic mucin was applied. In Experiment 5, "Commensal" and "Pathogenic" synthetic mucin samples (1.4% SF + 0.6% SF(D, E)-GalNAc, 1.4% SF + 0.6% SF(S)-GalN, and 2% SF) at 48 hours exhibited greater loss in monolayer integrity than samples at 24 hours. This was evidenced by the smaller

clumps of cells found in samples at 48 hours v. 24 hours (Figures 15 and 16). This difference was also observed for Experiments 6 and 7, but was even more pronounced in the latter. For Experiment 7, several 24-hour samples exhibited strong ZO-1 expression and pronounced chicken-wire patterns. However, the corresponding 48-hour samples were reduced to small clumps of cells. These differences in monolayer integrity for samples with synthetic mucin provided evidence that the synthetic mucins tested could not support the coexistence of Caco-2 cells and commensal bacteria or protect Caco-2 cells from compromise by pathogenic bacteria over an extended period (>48 hours). For “Pathogenic” samples containing synthetic mucin, previous research suggests that the Vat-AIEC protease secreted by AIEC could have played a role in mucin and monolayer breakdown. Studies have found that this protease can promote mucus degradation and the decrease of mucus viscosity, factors that allow AIEC to infiltrate mucus more easily [43]. The results of this study help establish a duration for how long silk-sugar synthetic mucins are expected to provide intestinal cells protection from bacteria infiltration. This can help inform how long future experiments on intestinal cells, synthetic mucin, and bacteria should last while still yielding desirable results.

5c. Positive Results

Although inconsistencies were found between results, some positive results were obtained throughout this study. Based on confocal images across multiple experiments, “2% SF” synthetic mucin to demonstrated to preserve Caco-2 monolayer integrity in the presence of commensal and pathogenic bacteria respectively. “2% SF” mucin effectiveness was demonstrated as early as Experiment 2, where the Commensal-2% SF sample exhibited strong ZO-1 expression and a defined chicken-wire pattern for the

Caco-2 monolayer (Figure 7). These traits of strong monolayer integrity were also identified in “2% SF” samples in Experiments 3, 4, and 6 across all bacteria groups (Figures 10, 12, and 18). “1.4% SF + 0.6% SF(D, E)-GalNAc” samples also exhibited Caco-2 monolayer preservation in the presence of bacteria, specifically in Experiments 4 and 6. Perhaps the best confocal results were obtained from Experiment 7 where, among 24-hour samples, all mucin groups demonstrated at least some ability to preserve monolayer integrity in the presence of bacteria (Figure 21). In this specific experiment, all synthetic mucins of silk-sugar composition demonstrated the ability to provide Caco-2 cells with an adequate barrier in the presence of pathogenic bacteria and/or the ability to maintain the co-existence of Caco-2 cells and commensal bacteria. Day 19 (24 hours’ post-bacteria application) TEER data supported these positive results (Figure 20), where TEER for most mucin groups was above 200 Ohms x cm^2, the minimum TEER associated with strong Caco-2 monolayer integrity [34].

The characteristics of strong ZO-1 expression and a defined chicken-wire pattern are standard features of fully differentiated, uncompromised Caco-2 monolayers seen in confocal images [55]. The presence of the O-glycans such as GalNAc and GalN in mucin samples containing SF(D, E)-GalNAc and SF(S)-GalN may have hindered bacteria proliferation and aided Caco-2 monolayer integrity in these samples. Previous research has suggested that inhibiting O-glycosylation of HT-29 cells improves the proliferation of commensal *E. coli* and changes their phenotype to become more pathogenic [56]. This research in part could explain why synthetic mucin groups at higher concentration (2% v. 5%) exhibited stronger barrier capacity, since the quantity of O-glycans would be greater in higher concentration samples. Synthetic mucins in the

present study may also have prevented bacteria infiltration by reducing bacteria biofilm formation. As mentioned in Section 2e, the synthetic mucins screened for this study originate from a study by Werlang et al., which investigated the influence of silk glycopolymers, such as SF-GalNAc and SF-GalN, on *Streptococcus* biofilm formation. SF(D, E)-GalNAc was created as a variant of SF(S)-GalNAc with 6-8 times lower GalNAc substitution. 4.5 wt % SF(D, E)-GalNAc and SF(S)-GalNAc reduced *S. mutans* biofilm formation by 83% and 96% respectively and without a killing effect. The study revealed that SF-GalNAc, rather than acting as a physical barrier, uses GalNAc to alter bacterial phenotype away from a biofilm-forming phenotype. *S. mutans* synthesizes exopolysaccharides to embed in an extracellular matrix and develop a biofilm. SF(S)-GalNAc induced bacteria to produce less exopolysaccharides, thus limiting biofilm development [51]. In the present study, perhaps SF(S)-GalNAc and SF(D, E)-GalNAc samples preserved Caco-2 monolayer integrity and prevented buildup of *E. coli* on monolayers through this mechanism. In the study by Werlang et al. SF-GalNAc polymers also exhibited greater biofilm reduction at higher concentrations (0.5%, 1.1%, and 2.25% v. 4.5%) [51]. In the present study, this could explain why the 5% synthetic mucins performed better than the 2% synthetic mucins in terms of monolayer preservation. Lastly, in the study by Werlang et al., SF(S)-GalNAc was shown to reduce biofilm formation without impacting bacteria growth in both commensal and pathogenic *Streptococcus* [51]. Based on this finding, the co-existence of Caco-2 cells and commensal *E. coli* may have been preserved in mucin samples containing SF(S)-GalNAc and SF(D, E)-GalNAc in the present study.

In the present study, “2% SF” and “5% SF” samples from “Commensal” and “Pathogenic” bacteria groups also exhibited evidence of Caco-2 monolayer preservation. On its own, silk fibroin (SF) biomaterials have been shown to support bacteria proliferation and biofilm formation. Therefore, SF biomaterials are often supplemented with antibiotics or inorganic nanomaterials that confer antimicrobial properties [58]. However, solubilized aqueous SF, which was used in the present study, has inherent antimicrobial properties. A study by Egan et al. revealed convincing evidence of these properties. In that study, SF solutions between 1-5% concentration were shown to significantly reduce the colony numbers of *Streptococcus aureus* and *Pseudomonas aeruginosa* bacteria, with higher concentrations (4-5%) completely preventing bacteria growth and colony formation. After finding that bacteria exposed to 100% water remained viable, they posited that SF may alter water activity by decreasing the amount of “free” water and reducing water activity by bacteria below a threshold. The researchers also exposed SF pads in LB agar plates to *S. aureus* and *P. aeruginosa*. They revealed that SF neither decreased nor increased bacteria growth significantly, suggesting that silk fibroin is bacteriostatic rather than bactericidal. In other words, SF prevents the growth of bacteria without killing the bacteria. Through live/dead imaging, Egan et al. also revealed that *S. aureus* and *P. aeruginosa* pre-exposed to SF could not form colonies on LB agar despite maintaining their plasma membranes after SF exposure. Based on subsequent zeta-potential measurements, it was suggested that SF altered the surface charge of these bacteria plasma membranes which could have influenced membrane permeability and ultimately inhibit bacteria growth. Ultimately, this study revealed the bacteriostatic nature of SF and how SF is more

capable at higher concentration [59]. Results from that study may provide evidence as to why 2-5% SF samples in the present study were able to prevent *E. coli* bacteria infiltration and maintain Caco-2 monolayer integrity.

The positive results of the present study are significant for providing quantitative and imaging data that demonstrates the effectiveness of silk/sugar synthetic mucins in preserving intestinal cell monolayer integrity in the presence of bacteria. Research by Werlang et al. and Egan et al. provide evidence of the potential mechanisms by which SF-sugar and SF synthetic mucins interact with bacteria. These results can help spur further development of silk-sugar synthetic mucins to the point that they reliably protect intestinal cells in bacteria presence while incorporating physical and chemical properties of native human intestinal mucus.

5d. Inconsistencies across Experiments

For this study, synthetic mucins were created primarily to mimic the barrier function of native human mucus. While positive results were obtained that suggested synthetic mucins could serve this function, results were also inconsistent and lead to conflicting conclusions. Synthetic mucin barrier function was assessed using TEER measurements and confocal imaging, as well as SEM imaging in earlier experiments. Generally, synthetic mucins exhibited similar barrier strength in the presence of commensal bacteria and pathogenic bacteria respectively. Among the bacteria-containing samples of Experiments 1 and 2, only the Commensal-2% SF samples of Experiment 2 exhibited strong ZO-1 expression and chicken-wire patterns (Figures 4 and 6). However, no Caco-2 monolayers were visible in the corresponding SEM images (Figures 5 and 8). Identical mucin groups were tested in Experiments 2 and 3. However,

unlike SEM imaging in Experiment 2, confocal imaging in Experiment 3 revealed strong ZO-1 expression and a chicken-wire pattern for the “Commensal” and “Pathogenic” synthetic mucin samples (Figures 8 and 10). From Experiments 4-7, synthetic mucins composed of silk-conjugated with sugar such as “1.4% SF + 0.6% SF(S)-GalNAc”, “1.4% SF + 0.6% SF(D, E)-GalNAc”, and “1.4% SF + 0.6% SF(S)-GalN” were tested against groups containing no synthetic mucin, porcine mucin, and pure silk fibroin. In Experiment 4, confocal and SEM imaging revealed Caco-2 monolayer formation for the “Commensal” synthetic mucin groups (“1.4% SF + 0.6% SF(S)-GalN”, “1.4% SF + 0.6% SF(D, E)-GalNAc”, and “2% SF”) (Figures 12 and 13). However, these same “Commensal” synthetic mucin groups did not exhibit strong Caco-2 monolayer formation under confocal imaging in the following Experiment 5 and Experiment 6 (Figures 15 and 18).

These comparisons in data highlight the general inconsistency in results between experiments. There were multiple sources of error that could have contributed to these inconsistencies and lead to undesirable results; results that exhibited how synthetic mucins could not protect intestinal cells from bacteria penetration. However, changes in experimental design were made to improve results and overcome challenges with each experiment. In the first 4 experiments, variability in silk batching may have contributed to inconsistencies between results. In this study, synthetic mucins were created from aqueous silk fibroin (SF) solutions. SF solutions are created from batches of *Bombyx mori* silk cocoons. The resulting batches of silk solution can vary in quality depending on a number of factors. Silk solution quality is dependent on where silk cocoons are sourced, how well SF is purified, the amount of solution being prepared at once, the age

of the silk solution, and overall how the silk solution is prepared [54]. These factors all introduce variation between batches of aqueous SF, even if they have the same concentrations. In the first 4 experiments, synthetic mucins could have been sourced from multiple batches of SF resulting in batch variation of SF solutions. This may have led to inconsistent SF quality between synthetic mucins within the same experiment. This batch variation could also still affect silk-sugar synthetic mucin components such as SF(D, E)-GalNAc, since the conjugation of SF and GalNAc is performed after aqueous SF is already prepared [37]. Results may also have been affected by the improper preparation of samples for imaging. During the confocal and SEM preparation of samples, transwells were rinsed several times and peeled off their transwell inserts using sharp tweezers. Improper handling of transwells using tweezers and aggressive aspiration during rinsing can cause trauma to transwells, removing Caco-2 cells that were already fixed. For example, this could explain the discrepancy of results in the confocal and SEM images of Experiment 2. Control-No mucin and Commensal-1.2% SF + 0.8% SF(S)-GalNAc samples exhibited decent Caco-2 monolayer formation. However, the corresponding SEM samples exhibited no monolayer formation.

5e. Challenges in Experimental Design

Sample Size

A significant issue that carried over across all experiments was the sizeable standard deviation in TEER found within replicate groups. These standard deviations are represented as error bars on TEER graphs. Overlapping error bars between mucin groups at a given time point were commonplace across experiments. Overlapping error bars between time points for a give mucin group were also common. Large error bars

made it difficult to draw comparisons between mucin groups and between time points. For example, in Experiment 4, Commensal-2% SF TEER decreased from Day 22 to Day 23. However, this decrease was not significant due to the large standard deviation of TEER for this group on Day 22. Findings like these made it more difficult to make solid claims about trends in data. Large standard deviation in mucin groups could be attributed to the sample size (number of replicates) in experiments. 3-5 replicates for every mucin group within each bacteria group were used to determine average TEER. Having more replicates per mucin group could have reduced the standard deviation size. In future experiments, having twice as many replicates, perhaps 6-10 replicates for every mucin group, could help make TEER data more reliable. The limited number of replicates used in these experiments also meant that data points that would be considered outliers could not be excluded from average TEER calculations. Excluding even a single replicate would significantly impact sample size that is already small.

Measuring TEER preceding Synthetic Mucin Application

Section 3f describes a change made in determining mucin application timing for the final 2 experiments. For the first 5 experiments, mucin was applied to transwells once Caco-2 cells were 100% confluent based on observation through a lab microscope. This procedure was used to assess when Caco-2 monolayers were at full strength. However, for the final 2 experiments, TEER instead was used to determine when Caco-2 monolayers in transwells reached full strength and to know when mucin should be applied. This change was made to reduce the impact of cell proliferation and differentiation on TEER measurements once synthetic mucin was applied. If mucin application was mistimed, TEER could increase or decrease independent of the

presence of synthetic mucin. In Experiment 2, for example, TEER decreases in “Control” and “Commensal” groups after mucin is applied and even before bacteria is applied (Figure 4). According to literature, Caco-2 cells typically require 21 days of cell culture on 24-well plate transwell inserts to form tight Caco-2 monolayers [44]. At this stage, Caco-2 cells would be fully differentiated and TEER for Caco-2 cells would be at its highest. However, TEER has also been observed to plateau between 15 and 21 days post-transwell seeding [45]. For the final 2 experiments, TEER was measured several days leading up to mucin application so that mucin could be applied when TEER began to plateau. It was predicted that TEER would plateau and maintain consistently high values for at least the duration of the experiment (4 days). This procedure was implemented to eliminate the effects on TEER from monolayers not being fully differentiated (TEER increasing independent of mucin or bacteria) or over-confluent (TEER decreasing independent of mucin or bacteria).

Timing Between Synthetic Mucin and Bacteria Application

Another potential source of error for results was the inconsistency in timing between synthetic mucin application and bacteria application. In some experiments, synthetic mucin and bacteria were applied 2 days apart rather than 1 day apart. The differences in time between mucin and bacteria application were not a concern initially. However, only in the final 2 experiments was it realized that needlessly adding extending time between mucin and bacteria applications could cause TEER to fall out of its “plateau range” during the experiments. A couple other issues may have led to inconsistent results. In the first 4 experiments, silk may have been sourced from different batches, which could have led to inconsistency in the quality of silk when

creating synthetic mucins. In the later experiments, synthetic mucins were created from the same batch of silk to eliminate inconsistency in silk quality. Additionally, results in Experiment 5 may have been affected by incubating Caco-2 cells in a malfunctioning cell incubator. In this instance, the Caco-2 cells may have incubated below 5% CO_2 after transwell seeding. 5% CO_2 during incubation is meant to maintain the pH of growth media within a physiological range [46]. If CO_2 drops too low, growth media pH becomes too alkaline and this can cause cell mutations and cell death [47].

Immunostaining Challenges

In the “Permeabilization, Blocking, and Antibody Staining” sub-section of Section 3h, a change in immunostaining procedure is described. For all but the final experiment, transwell membranes were excised from their transwell inserts using a sharp tweezer and placed into 96-well plates. This was done to save time while performing the remaining immunostaining steps. However, it was observed that excising and handling transwells with tweezers could cause cell trauma. Removing transwell membranes from their inserts involved the puncturing and shearing of transwells. This process resulted in many cells being lost either by being flung off or rubbed off the membranes. Caco-2 monolayer integrity would be disrupted as a result and clumps of cells would be separated, even though this step was performed after fixation. To eliminate the use of tweezers, transwells membranes were kept intact within transwell inserts for remaining permeabilization, blocking, and antibody staining steps in Experiment 7. Additionally, Caco-2 cells on membranes excised from inserts would often become dislodged from aspiration during immunostaining, even when attempting to aspirate carefully. However, keeping transwell membranes intact also mitigated this impact of aspiration.

6. Future Directions

This study was unable to identify a synthetic mucin that could provide a sufficient physical barrier between intestinal cells and bacteria and support the co-culture of intestinal cells and commensal bacteria. However, the need for a more comprehensive and biologically relevant *in vitro* intestinal models persists and so the hunt for a synthetic mucin that satisfies the objectives of this study continues. Future investigations towards ideal synthetic mucins could benefit from the improvements in experimental design outlined in Section 5e. Executing these improvements should yield more reliable data if these experiments are repeated in the future.

Screening Synthetic Mucin Effectiveness with Different Bacteria

This study used commensal and pathogenic strains of *E. coli* to test the effectiveness of synthetic mucins. Results on whether synthetic mucins serve as effective barriers is still under investigation. However, perhaps the silk-sugar synthetic mucins from this study could prove effective against other types of bacteria. In a previous study, the effectiveness of SF(S)-GalNAc and SF(D, E)-GalNAc against *Streptococcus mutans* (*S. mutans*), a pathogenic bacteria found in the oral cavity, was proven. In that study, 4.5 wt% SF(S)-GalNAc and SF(D, E)-GalNAc reduced *S. mutans* biofilm formation by 96% and 83% respectively in an *in vitro* oral cavity model [37].

Co-culturing Commensal and Pathogenic Bacteria

Further optimizations could be made to improve the barrier function of synthetic mucin and these optimizations could be investigated in future studies. In the present study, the co-culture of intestinal epithelial cells with commensal and pathogenic strains

of bacteria respectively was studied. If synthetic mucin was identified that could fulfill the main goals of this study, further research could focus on the co-culture of intestinal cells with both commensal and pathogenic strains. Such studies could reveal whether synthetic mucin would support both commensal and pathogenic bacteria strains without compromising intestinal cell monolayer integrity. The EcN and AIEC *E. coli* strains used in the present study could be used on this front. EcN has been shown to provide protective benefits for intestinal epithelial cells against AIEC. EcN can directly stimulate beta-defensin production, which can impede the adhesion and invasion of the cells by AIEC [48]. These future studies on bacteria co-culture could toggle the ratios of commensal to pathogenic bacteria to learn what ratios intestinal cells tolerate, but also what ratios provide a protective benefit for intestinal cell integrity.

Synthetic Mucin Supplementation by AMPs

In future studies, researchers could also test synthetic mucin supplementation with antimicrobial peptides (AMPs). AMP α-defensin 5 (HD5) has especially been demonstrated to be effective at combating pathogenic bacteria. α-defensins like HD5 have been shown to protect against Gram-negative bacteria and be effective against several types of bacteria, including *E. coli* [49]. HD5 is especially interesting since it is one of two α-defensins produced in specifically by Paneth cells in intestinal crypts. Thus, the incorporation of HD5 in synthetic mucin could also help improve the biological relevance of synthetic mucins. Other AMPs found in the human gastrointestinal tract such as Reg3 lectins and galectins also combat bacteria. Reg3 lectins have been shown to selectively target gram-positive bacteria. Galectin-4 and Galectin-8 have been shown to specifically target *E. coli* that mimic antigens found in human blood [50].

Tuning Synthetic Mucin Viscosity

The effectiveness of different synthetic mucin concentrations was investigated in this study. Synthetic mucin concentrations ranging from 0.5-5% are considered biologically relevant since they match the concentrations of MUC2 in small intestinal mucus. Little emphasis, however, was placed on whether the mucins of the present study matched the rheological properties of native human mucus. For experiments in this study that tested porcine mucin, it was observed that porcine mucin, despite matching concentrations of other synthetic mucins, was notably more viscous and became more viscous at higher concentrations (2% versus 5%). Samples with 2% porcine mucin exhibited noticeably worse Caco-2 monolayer integrity than synthetic mucin samples, perhaps due the high relative viscosity of porcine mucin. Matching the viscosity of synthetic mucins to that of native intestinal mucus could improve the biological relevance of these mucins. In the study by Werlang et al., where the silk-sugar polymers used in the present study were developed, viscosities of these polymers were verified. In that study, 4.5% SF, SF(S)-GalNAc, SF(D, E)-GalNAc, and SF(S)-GalN had viscosities ranging from 50-100 mPA•s at 1 s^{-1} shear rate to 2-6 mPa•s at 90 s^{-1} shear rate [51]. Human intestinal mucus viscosity ranges from 1-25 mPa•s according to Larhed et al., although shear rates were not specified [60]. Therefore, viscosities found in the study by Werlang et al. may have been biologically relevant. However, because most experiments in the present study tested 2% silk-sugar mucins instead of 4.5% silk-sugar mucins, the viscosities by Werlang et al. may not have been relevant for the present study. In polymer solutions, viscosity decreases as concentration decrease [61]. Perhaps results in the present study were less convincing at lower concentration (2% v.

5%) because synthetic mucins were not viscous enough to form hydrogels. Synthetic mucins also may have had difficulty maintaining hydrogel structure in the presence of Caco-2 media underneath transwells and bacteria-containing media above the mucins. These realizations further necessitate investigation of the rheological properties of synthetic mucins in future experiments.

Synthetic Mucin Impact on Cell Development

This study focused on the interactions between synthetic mucin and bacteria and whether synthetic mucin could have provide intestinal cells protection from bacteria. However, the influence synthetic mucin had on intestinal cell proliferation and differentiation was not thoroughly investigated. For the experiments in this study, synthetic mucin was always applied once intestinal cells were already 100% confluent. Separate studies not involving bacteria could be performed where synthetic mucin could be applied much closer to start of cell seeding. In these experiments, cells were seeded at 10% confluence and were not fully differentiated. If synthetic mucin were applied perhaps 1-2 days post-seeding, the influence of synthetic mucin on the cell development could be studied with more depth. Additionally, the mechanisms by which silk-sugar mucins benefit Caco-2 monolayer integrity were not sufficiently elucidated. During experiments, synthetic mucin groups that did not contain Caco-2 cells were not included. If testing was done on groups without Caco-2 cells, whether TEER could increase solely due to synthetic mucin presence or if TEER increased due to an interaction between Caco-2 cells and synthetic mucins that modified the properties of the cells could have been assessed.

Confirming Synthetic Mucin Compatibility with Complex in vitro Models

Work on screening synthetic mucins that are compatible with Caco-2 cells and can fulfill the primary goals of this experiment is ongoing. However, if successful synthetic mucin candidates are identified, the next steps would be to confirm if these candidates are compatible with more complex *in vitro* intestinal epithelial models. This study focused on screening with a 2D *in vitro* intestinal epithelial model with Caco-2 cells. Future screening, however, could be performed on the equivalent model with organoids. To reiterate, Caco-2 cells instead of organoids were used in this study because the latter were less resilient to cell culture and more expensive to maintain. However, organoids are markedly more biological relevant than Caco-2 cells to native intestinal epithelial cells because of their 3D structure and ability to differentiate into numerous epithelial cell types. Synthetic mucins successfully screened with organoids could then be incorporated into 3D *in vitro* models such as the 3D half-scaffold model developed by Kaplan laboratory.

Vitality of Synthetic Mucin Assessments

In the present study, confocal data often yielded more promising results than TEER data, providing evidence that synthetic mucins could maintain Caco-2 monolayer integrity in bacteria presence. This relationship between TEER and confocal data was especially present in earlier experiments. However, TEER should still be considered the primary screening tool for assessing synthetic mucin capability moving forward. In the present study, confocal samples were imaged based on how they compared to other samples within the same mucin and bacteria groups. Confocal images of multiple replicates were taken, however, the replicate exhibiting the strongest Caco-2 monolayer

integrity would ultimately be chosen as a representative for the mucin group overall. Additionally, Caco-2 images are taken of only a section of the whole transwell membrane. In contrast, TEER data was taken as an average of multiple replicates. Thus, TEER data is more comprehensive and more dependable than confocal data. Confocal data is still significant, but should be considered supplemental data that confirms TEER data.

7. Conclusion

Numerous *in vitro* models of the small intestinal epithelium have been created to improve overall understanding of the small intestine. These models, such as the 3D models produced by Kaplan laboratory, have improved understanding by studying the development and differentiation of intestinal epithelial cells, intestinal disease pathogenesis caused by harmful microbes, the interactions between intestinal cells and microbiota, and much more. These models use Caco-2 cells, HT-29 MTX cells, and intestinal epithelial organoids to model the intestinal epithelium. However, these cell types are unable to produce a high yield of mucus, sufficient enough to mimic the protective barrier and microbe co-existence functions of native intestinal mucus. Synthetic mucins and animal-derived mucus have been used to address the issue of low yield. However, these previously-developed mucus has limited biological relevance to native human intestinal mucus. Thus, this study attempted to address the need for biologically relevant synthetic mucin that can provide intestinal cells with protection from pathogenic bacteria and can support the co-culture of intestinal cells and commensal bacteria. This study employed TEER measurements, confocal imaging, and SEM imaging as tools for screening synthetic mucins of silk-sugar composition against commensal (EcN) and pathogenic (AIEC) *E. coli*. Results somewhat demonstrated that synthetic mucins of silk-sugar composition could maintain Caco-2 monolayer integrity in the presence of commensal and pathogenic *E. coli*. However, results on this ability conflicted between experiments. Thus, further research is required to reliably validate the ability of silk-sugar synthetic mucins to mimic native human intestinal mucus. This study also established a protocol for screening synthetic mucins in an 2D transwell

platform. Improvements in experimental design were discovered during this study and such improvements can be implemented in future synthetic mucin screening. Additionally, there is room for further optimization of synthetic mucins by, for example, testing mucin efficacy on other genus of bacteria, supplementing mucin with AMPs, and tuning mucin rheological properties. Ultimately, successful optimization and incorporation of synthetic mucins into more complex 3D *in vitro* intestinal epithelial models could advance understanding of the human small intestine.

8. References

1. Kim, Y., Pritts, T.A. (2017). The Gastrointestinal Tract. In: Luchette, F., Yelon, J. (eds) Geriatric Trauma and Critical Care. Springer, Cham. https://doi.org/10.1007/978-3-319-48687-1_5

2. Kastl, A. J., Jr, Terry, N. A., Wu, G. D., & Albenberg, L. G. (2020). The Structure and Function of the Human Small Intestinal Microbiota: Current Understanding and Future Directions. Cellular and molecular gastroenterology and hepatology, 9(1), 33–45. https://doi.org/10.1016/j.jcmgh.2019.07.006

3. Mahadevan, V. (2020). Anatomy of the small intestine. Surgery (Oxford), 38(6), 283–288. https://doi.org/10.1016/j.mpsur.2020.03.012

4. Hansson G. C. (2012). Role of mucus layers in gut infection and inflammation. Current opinion in microbiology, 15(1), 57–62. https://doi.org/10.1016/j.mib.2011.11.002

5. Allaire, J. M., Crowley, S. M., Law, H. T., Chang, S.-Y., Ko, H.-J., & Vallance, B. A. (2018). The intestinal epithelium: Central Coordinator of mucosal immunity. Trends in Immunology, 39(9), 677–696. https://doi.org/10.1016/j.it.2018.04.002

6. Shreiner, A. B., Kao, J. Y., & Young, V. B. (2015). The gut microbiome in health and in disease. Current opinion in gastroenterology, 31(1), 69–75. https://doi.org/10.1097/MOG.0000000000000139

7. Hansson, G. C. (2020). Mucins and the microbiome. Annual Review of Biochemistry, 89(1), 769–793. https://doi.org/10.1146/annurev-biochem-011520-105053

8. Lock, J. Y., Carlson, T. L., & Carrier, R. L. (2018). Mucus models to evaluate the diffusion of drugs and particles. Advanced drug delivery reviews, 124, 34–49. https://doi.org/10.1016/j.addr.2017.11.001

9. Bowcutt, R., Forman, R., Glymenaki, M., Carding, S. R., Else, K. J., & Cruickshank, S. M. (2014). Heterogeneity across the murine small and large intestine. World journal of gastroenterology, 20(41), 15216–15232. https://doi.org/10.3748/wjg.v20.i41.15216

10. Ermund, A., Schütte, A., Johansson, M. E., Gustafsson, J. K., & Hansson, G. C. (2013). Studies of mucus in mouse stomach, small intestine, and colon. I. Gastrointestinal mucus layers have different properties depending on location as well as over the Peyer's patches. American journal of physiology. Gastrointestinal and liver physiology, 305(5), G341–G347. https://doi.org/10.1152/ajpgi.00046.2013

11. Bansil, R., & Turner, B. S. (2018). The biology of mucus: Composition, synthesis and organization. Advanced drug delivery reviews, 124, 3–15. https://doi.org/10.1016/j.addr.2017.09.023

12. Bansil, R., & Turner, B. S. (2006). Mucin structure, aggregation, physiological functions and biomedical applications. Current Opinion in Colloid & Interface Science, 11(2-3), 164–170. https://doi.org/10.1016/j.cocis.2005.11.001

13. Boegh, M., & Nielsen, H. M. (2015). Mucus as a barrier to drug delivery – understanding and mimicking the barrier properties. Basic & clinical pharmacology & toxicology, 116(3), 179–186. https://doi.org/10.1111/bcpt.12342

14. Taylor, C., Allen, A., Dettmar, P. W., & Pearson, J. P. (2003). The gel matrix of gastric mucus is maintained by a complex interplay of transient and nontransient associations. Biomacromolecules, 4(4), 922–927. https://doi.org/10.1021/bm025767t

15. Round, A. N., Rigby, N. M., Garcia de la Torre, A., Macierzanka, A., Mills, E. N., & Mackie, A. R. (2012). Lamellar structures of MUC2-rich mucin: a potential role in governing the barrier and lubricating functions of intestinal mucus. Biomacromolecules, 13(10), 3253–3261. https://doi.org/10.1021/bm301024x

16. Witten, J., Samad, T., & Ribbeck, K. (2018). Selective permeability of mucus barriers. Current opinion in biotechnology, 52, 124–133. https://doi.org/10.1016/j.copbio.2018.03.010

17. Wang, B. X., Wu, C. M., & Ribbeck, K. (2021). Home, sweet home: how mucus accommodates our microbiota. The FEBS journal, 288(6), 1789–1799. https://doi.org/10.1111/febs.15504

18. Tailford, L. E., Crost, E. H., Kavanaugh, D., & Juge, N. (2015). Mucin glycan foraging in the human gut microbiome. Frontiers in genetics, 6, 81. https://doi.org/10.3389/fgene.2015.00081

19. Werlang, C., Cárcarmo-Oyarce, G., & Ribbeck, K. (2019). Engineering mucus to study and influence the microbiome. Nature Reviews Materials, 4(2), 134–145. https://doi.org/10.1038/s41578-018-0079-7

20. Hansson G. C. (2019). Mucus and mucins in diseases of the intestinal and respiratory tracts. Journal of internal medicine, 285(5), 479–490. https://doi.org/10.1111/joim.12910

21. Grubb, B. R., & Boucher, R. C. (1999). Pathophysiology of gene-targeted mouse models for cystic fibrosis. Physiological reviews, 79(1 Suppl), S193–S214. https://doi.org/10.1152/physrev.1999.79.1.S193

22. Johansson, M. E., Jakobsson, H. E., Holmén-Larsson, J., Schütte, A., Ermund, A., Rodríguez-Piñeiro, A. M., Arike, L., Wising, C., Svensson, F., Bäckhed, F., & Hansson, G. C. (2015). Normalization of Host Intestinal Mucus Layers Requires Long-Term Microbial Colonization. Cell host & microbe, 18(5), 582–592. https://doi.org/10.1016/j.chom.2015.10.007

23. Zweibaum, A., Pinto, M., Chevalier, G., Dussaulx, E., Triadou, N., Lacroix, B., Haffen, K., Brun, J. L., & Rousset, M. (1985). Enterocytic differentiation of a subpopulation of the human colon tumor cell line HT-29 selected for growth in sugar-free medium and its inhibition by glucose. Journal of cellular physiology, 122(1), 21–29. https://doi.org/10.1002/jcp.1041220105

24. Lozoya-Agullo, I., Araújo, F., González-Álvarez, I., Merino-Sanjuán, M., González-Álvarez, M., Bermejo, M., & Sarmento, B. (2017). Usefulness of caco-2/HT29-MTX and Caco-2/HT29-MTX/raji B coculture models to predict intestinal and colonic permeability compared to Caco-2 monoculture. Molecular Pharmaceutics, 14(4), 1264–1270. https://doi.org/10.1021/acs.molpharmaceut.6b01165

25. Wodzanowski, K. A., Cassel, S. E., Grimes, C. L., & Kloxin, A. M. (2020). Tools for probing host-bacteria interactions in the gut microenvironment: From molecular to cellular levels. Bioorganic & medicinal chemistry letters, 30(10), 127116. https://doi.org/10.1016/j.bmcl.2020.127116

26. Verhoeckx, K., Cotter, P., López-Expósito, I., Kleiveland, C., Lea, T., Mackie, A., Requena, T., Swiatecka, D., & Wichers, H. (Eds.). (2015). The Impact of Food Bioactives on Health: in vitro and ex vivo models. Springer.

27. Zweibaum, A., Laburthe, M., Grasset, E., & Louvard, D. (1991). Use of cultured cell lines in studies of intestinal cell differentiation and function. Comprehensive Physiology, 223–255. https://doi.org/10.1002/cphy.cp060407

28. Chen, Y., Lin, Y., Davis, K. et al. Robust bioengineered 3D functional human intestinal epithelium. Sci Rep 5, 13708 (2015). https://doi.org/10.1038/srep13708

29. Chen, Y., Zhou, W., Roh, T., Estes, M. K., & Kaplan, D. L. (2017). In vitro enteroid-derived three-dimensional tissue model of human small intestinal epithelium with innate immune responses. PloS one, 12(11), e0187880. https://doi.org/10.1371/journal.pone.0187880

30. Chen, Y., Rudolph, S. E., Longo, B. N., Pace, F., Roh, T. T., Condruti, R., Gee, M., Watnick, P. I., & Kaplan, D. L. (2022). Bioengineered 3D Tissue Model of Intestine Epithelium with Oxygen Gradients to Sustain Human Gut Microbiome. Advanced healthcare materials, 11(16), e2200447. https://doi.org/10.1002/adhm.202200447

31. Kim, H. J., Huh, D., Hamilton, G., & Ingber, D. E. (2012). Human gut-on-a-chip inhabited by microbial flora that experiences intestinal peristalsis-like motions and flow. Lab on a chip, 12(12), 2165–2174. https://doi.org/10.1039/c2lc40074j

32. Kramer, J. R., Onoa, B., Bustamante, C., & Bertozzi, C. R. (2015). Chemically tunable mucin chimeras assembled on living cells. Proceedings of the National Academy of Sciences of the United States of America, 112(41), 12574–12579. https://doi.org/10.1073/pnas.1516127112

33. Dekina, S., Romanovska, I., Ovsepyan, A., Tkach, V., & Muratov, E. (2016). Gelatin/carboxymethyl cellulose mucoadhesive films with lysozyme: Development and characterization. Carbohydrate polymers, 147, 208–215. https://doi.org/10.1016/j.carbpol.2016./04.006

34. Withington, L. (2002). High-throughput epithelial cell culture systems for screening drug intestinal permeability. CRC Press EBooks, 120–137. https://doi.org/10.1201/9780203219935-13

35. Sabboh-Jourdan, H., Valla, F., Epriliati, I., & Gidley, M. J. (2010). Organic acid bioavailability from banana and sweet potato using an in vitro digestion and Caco-2 cell model. European Journal of Nutrition, 50(1), 31–40. https://doi.org/10.1007/s00394-010-0112-0

36. Malpique, R., Ehrhart, F., Katsen-Globa, A., Zimmermann, H., & Alves, P. M. (2009). Cryopreservation of Adherent Cells: Strategies to Improve Cell Viability and Function After Thawing. Tissue Engineering Part C: Methods, 15(3), 373–386. https://doi.org/10.1089/ten.tec.2008.0410

37. Werlang, C. (2023). The regulation of bacterial virulence by mucin glycans (pp. 61–101). https://dspace.mit.edu/handle/1721.1/152450

38. Walter, E., & Kissel, T. (1995). Heterogeneity in the human intestinal cell line Caco-2 leads to differences in transepithelial transport. European Journal of Pharmaceutical Sciences, 3(4), 215–230. https://doi.org/10.1016/0928-0987(95)00010-b

39. Caco-2 [Caco2] | ATCC. (n.d.). Www.atcc.org. https://www.atcc.org/products/htb-37

40. Mélanie Kucki, Diener, L., Bohmer, N., Hirsch, C., Krug, H. F., Palermo, V., & Wick, P. (2017). Uptake of label-free graphene oxide by Caco-2 cells is dependent on the cell differentiation status. Journal of Nanobiotechnology, 15(1). https://doi.org/10.1186/s12951-017-0280-7

41. Schimpel, C., Birgit Johanna Teubl, Absenger, M., Meindl, C., Fröhlich, E., Gerd Leitinger, Zimmer, A., & Roblegg, E. (2014). Development of an Advanced Intestinal in Vitro Triple Culture Permeability Model To Study Transport of Nanoparticles. Molecular Pharmaceutics, 11(3), 808–818. https://doi.org/10.1021/mp400507g

42. Leal, J., Smyth, H. D. C., & Ghosh, D. (2017). Physicochemical properties of mucus and their impact on transmucosal drug delivery. International Journal of Pharmaceutics, 532(1), 555–572. https://doi.org/10.1016/j.ijpharm.2017.09.018

43. Zheng, L., Duan, S.-L., Dai, Y.-C., & Wu, S. (2022). Role of adherent invasive Escherichia coli in pathogenesis of inflammatory bowel disease. World Journal of Clinical Cases, 10(32), 11671–11689. https://doi.org/10.12998/wjcc.v10.i32.11671

44. Uchida, M., Fukazawa, T., Yamazaki, Y., Hashimoto, H., & Miyamoto, Y. (2009). A modified fast (4 day) 96-well plate Caco-2 permeability assay. Journal of Pharmacological and Toxicological Methods, 59(1), 39–43. https://doi.org/10.1016/j.vascn.2008.10.006

45. Ferruzza, S., Rossi, C., Scarino, M. L., & Sambuy, Y. (2012). A protocol for differentiation of human intestinal Caco-2 cells in asymmetric serum-containing medium. Toxicology in Vitro, 26(8), 1252–1255. https://doi.org/10.1016/j.tiv.2012.01.008

46. Cooper, J. (2019, August). CO2 concentration and pH control in the cell culture laboratory. Culture Collections. https://www.culturecollections.org.uk/culture-collection-news/co2-concentration-and-ph-control-in-the-cell-culture-laboratory/

47. pH Monitoring for Suspension Cultures - Scientific Bioprocessing. (n.d.). Www.scientificbio.com. https://www.scientificbio.com/ph-monitoring

48. Scaldaferri, F., Gerardi, V., Mangiola, F., Lopetuso, L. R., Pizzoferrato, M., Petito, V., Papa, A., Stojanovic, J., Poscia, A., Cammarota, G., & Gasbarrini, A. (2016). Role and mechanisms of action ofEscherichia coliNissle 1917 in the maintenance of remission in ulcerative colitis patients: An update. World Journal of Gastroenterology, 22(24), 5505. https://doi.org/10.3748/wjg.v22.i24.5505

49. Wehkamp, J., Fellermann, K., Herrlinger, K. R., Bevins, C. L., & Stange, E. F. (2005). Mechanisms of Disease: defensins in gastrointestinal diseases. Nature Clinical Practice Gastroenterology & Hepatology, 2(9), 406–415. https://doi.org/10.1038/ncpgasthep0265

50. Mukherjee, S., & Hooper, L. V. (2015). Antimicrobial Defense of the Intestine. Immunity, 42(1), 28–39. https://doi.org/10.1016/j.immuni.2014.12.028

51. Werlang, C. A., Sahoo, J. K., Cárcarmo-Oyarce, G., Stevens, C., Uzun, D., Putnik, R., Hasturk, O., Choi, J., Kaplan, D. L., & Ribbeck, K. (2024). Selective Biofilm Inhibition through Mucin-Inspired Engineering of Silk Glycopolymers. Journal of the American Chemical Society, 146(50), 34661–34668. https://doi.org/10.1021/jacs.4c12945

52. Novus Biologicals, LLC. (2020). MUC2 Antibody (CCP58). Novus Biologicals. https://www.novusbio.com/products/muc2-antibody-ccp58_nbp2-25221

53. DAPI (4’,6-diamidino-2-phenylindole) - US. (n.d.). Www.thermofisher.com. https://www.thermofisher.com/us/en/home/life-science/cell-analysis/fluorophores/dapi-stain.html

54. Rockwood, D. N., Preda, R. C., Yücel, T., Wang, X., Lovett, M. L., & Kaplan, D. L. (2011). Materials fabrication from Bombyx mori silk fibroin. Nature protocols, 6(10), 1612–1631. https://doi.org/10.1038/nprot.2011.379

55. Hiebl, V., Schachner, D., Ladurner, A., Heiss, E. H., Stangl, H., & Dirsch, V. M. (2020). Caco-2 Cells for Measuring Intestinal Cholesterol Transport - Possibilities and Limitations. Biological Procedures Online, 22(1). https://doi.org/10.1186/s12575-020-00120-w

56. Wei, J., Chen, C., Feng, J., Zhou, S., Feng, X., Yang, Z., Lu, H., Tao, H., Li, L., Xv, H., Xuan, J., & Wang, F. (2023). Muc2 mucin o-glycosylation interacts with enteropathogenic Escherichia coli to influence the development of ulcerative colitis based on the NF-kB signaling pathway. Journal of Translational Medicine, 21(1). https://doi.org/10.1186/s12967-023-04687-2

57. Measurement of Transepithelial Electrical Resistance (TEER). (n.d.). Ebrary. https://ebrary.net/24380/health/measurement_transepithelial_electrical_resistance_teer

58. Ghalei, S., & Handa, H. (2022). A review on antibacterial silk fibroin-based biomaterials: current state and prospects. Materials Today Chemistry, 23, 100673. https://doi.org/10.1016/j.mtchem.2021.100673

59. Egan, G., Hannah, A. J., Donnelly, S., Connolly, P., & Seib, F. P. (2024). The Biologically Active Biopolymer Silk: The Antibacterial Effects of Solubilized Bombyx mori Silk Fibroin with Common Wound Pathogens. Advanced Biology, 8(5). https://doi.org/10.1002/adbi.202300115

60. Larhed, A. W., Artursson, P., Gråsjö, J., & Björk, E. (1997). Diffusion of Drugs in Native and Purified Gastrointestinal Mucus. Journal of Pharmaceutical Sciences, 86(6), 660–665. https://doi.org/10.1021/js960503w

61. Schaller, C. (2019, October 1). 4.2: Viscosity of Polymers. Chemistry LibreTexts. https://chem.libretexts.org/Bookshelves/Organic_Chemistry/Polymer_Chemistry_(Schaller)/04%3A_Polymer_Properties/4.02%3A_Viscosity

62. ZO-1 Monoclonal Antibody (ZO1-1A12), Alexa FluorTM 594 (339194). (2024). Thermofisher.com. https://www.thermofisher.com/antibody/product/ZO-1-Antibody-clone-ZO1-1A12-Monoclonal/339194